

## Research paper

## Structure-activity relationships reveal a 4-(2-pyridyl)chalcone as a potent cell death inducer

Juan Perdomo<sup>a</sup>, Henoc del Rosario<sup>a</sup>, Ester Saavedra<sup>a</sup>, Mercedes Said<sup>a</sup>, Celina García<sup>b</sup>,  
Lía Cruces<sup>c,d</sup>, Susana Abdala<sup>c</sup>, Ignacio Brouard<sup>d</sup>, José Quintana<sup>a</sup>, Francisco Estévez<sup>a,\*</sup>

<sup>a</sup> Departamento de Bioquímica y Biología Molecular, Fisiología, Genética e Inmunología, Instituto Universitario de Investigaciones Biomédicas y Sanitarias (IUIBS), Grupo de Química Orgánica y Bioquímica, Universidad de Las Palmas de Gran Canaria, Unidad Asociada al Consejo Superior de Investigaciones Científicas (CSIC), 35016, Las Palmas de Gran Canaria, Spain

<sup>b</sup> Instituto Universitario de Bio-Organica "Antonio González" (IUBO-AG), Departamento de Química Orgánica, Universidad de La Laguna, La Laguna, Tenerife, Spain

<sup>c</sup> Departamento de Medicina Física y Farmacología, Facultad de Farmacia, Universidad de La Laguna, Tenerife, Spain

<sup>d</sup> Instituto de Productos Naturales y Agrobiología, Consejo Superior de Investigaciones Científicas (IPNA-CSIC), 38206, La Laguna, Tenerife, Spain

## ARTICLE INFO

## Keywords:

Apoptosis  
Caspase  
Cell cycle  
Chalcone  
Cytotoxicity

## ABSTRACT

Chalcones are biosynthetic precursors of flavonoids and are considered potential anticancer drugs. Here, twenty-two chalcones were synthesized and evaluated for their effects on the viability of eight human leukaemia cells. This series of chalcones was characterized by the presence or absence of a benzyloxy group on the A ring and one or two substituents on the B ring including halogen, methoxy, trifluoromethyl, benzyloxy, morpholine and pyridine in the chalcone skeleton. Chalcones with the lowest IC<sub>50</sub> values against leukaemia cells contained a benzyloxy group at position 2' on the A ring and one or two halogens, or a 2-pyridyl group at position 4 on the B ring. The chalcone 6'-benzyloxy-2'-hydroxy-4-(2-pyridyl)chalcone (BHP) exhibited potency comparable to the antitumor agent etoposide against U-937 cells while showing lower toxicity against human peripheral blood mononuclear cells. BHP-induced viability inhibition was not linked to cell cycle arrest but was associated with apoptosis. Overexpression of the antiapoptotic protein Bcl-2 and the P-glycoprotein did not prevent its activity. In U-937 and HL-60 cells, BHP triggered mitochondrial cytochrome c release, activation of caspases and poly (ADP-ribose) polymerase cleavage and increased annexin-V positive cells. Cell death triggered by BHP was (i) blocked by a pan-caspase inhibitor and by a specific caspase-9 inhibitor, (ii) associated with the phosphorylation of the mitogen-activated protein kinases and (iii) dependent of the generation of reactive oxygen species.

## 1. Introduction

Leukaemia is used to reference a broad array of hematopoietic malignancies characterized by excess white blood cells in the bloodstream [1]. It is the most common childhood cancer however the majority of patients (93 %) are diagnosed at age 20 years and older [2]. Leukaemia is classified using two criteria: (i) myeloid or lymphoid lineage and (ii) acute or chronic. The latter refers to the speed of clinical onset [3]. The most common leukaemias among children and adolescents are acute lymphocytic leukaemia/lymphoma, whereas acute myeloid leukaemia, chronic myeloid leukaemia and chronic lymphocytic leukaemia/small lymphocytic lymphoma are much more common in older adults [3]. Acute and chronic myeloid leukaemias are clonal haematologic malignancies driven by key mutations arising in hematopoietic stem cells and

myeloid progenitors [4]. The first-line treatment for acute myeloid leukaemia has remained largely unchanged for the past fifty years [5]. However, since 2017, nine agents—including several targeted therapies—have been approved for this disease [6]. Although many patients achieve complete remission, approximately half experience relapse. According to cancer survivorship statistics published in 2025, the 5-year relative survival rate is 70 % for children and adolescents but declines to 11 % for patients aged 65 years and older [7]. Many chronic myeloid leukaemia patients have benefitted from tyrosine kinase inhibitors, which improve the 5-year survival rate to above 80 % [8]. This survival rate may drop to 20 % if chronic myeloid leukaemia changes from chronic phase to blast phase [9]. According to the GLOBOCAN database, the estimated global incidence and mortality from leukaemia in 2022 were 487,294 and 305,405 cases, respectively. These figures underscore

\* Corresponding author.

E-mail address: [francisco.estevez@ulpgc.es](mailto:francisco.estevez@ulpgc.es) (F. Estévez).

<https://doi.org/10.1016/j.cbi.2025.111877>

Received 26 September 2025; Received in revised form 15 November 2025; Accepted 11 December 2025

Available online 13 December 2025

0009-2797/© 2025 The Authors. Published by Elsevier B.V. This is an open access article under the CC BY license (<http://creativecommons.org/licenses/by/4.0/>).

that mortality rates for these haematological malignancies remain high [10] which highlights the urgent need for novel therapies to improve treatment efficacy.

Despite new-targeted therapies against haematological malignancies the appearance of resistance mechanisms is one of the main limitations. Resistance to cell death is considered a core hallmark of cancer and represents a severe problem in clinical management [11,12]. Apoptotic cell death is a form of regulated cell death mediated by aspartate-specific cysteine proteases of the caspase family [13]. Two major signalling pathways initiate apoptosis: the intrinsic and extrinsic pathways [14]. The intrinsic or mitochondrial pathway is initiated by microenvironmental perturbations, and characterized by increased permeability of the mitochondrial outer membrane, leading to the cytosolic release of proapoptotic factors, sequential activation of the initiator caspase-9, and then executioner caspases, caspase-3 and caspase-7 [14]. The extrinsic pathway is initiated by death receptors upon binding to their cognate ligands, leading to caspase-8 activation and subsequent proteolytic activation of executioner caspases, primarily caspase-3 [15].

There is growing interest in identifying chemical entities inspired by naturally occurring compounds as potential novel anti-cancer agents, particularly for haematological malignancies [16]. Plant flavonoids, secondary metabolites with a wide range of biological activities [17], are polyphenolic compounds that modulate multiple signal transduction pathways involved in angiogenesis, proliferation, metastasis, and apoptosis [18]. Chalcones, 1,3-diphenyl-2-propen-1-one derivatives, can be considered flavonoids with an open-chain structure. Both naturally occurring and synthetic chalcones exhibit diverse biological activities, including significant cytotoxicity against various cancer cell types while sparing normal human cells [19–21]. The chalcone scaffold serves as a central framework for introducing simple substituents with minimal synthetic steps. Recent efforts have focused on designing chalcones that can be synthesized efficiently, interact effectively with biological targets, and comply with principles of functional synthesis and green chemistry [22]. In this study, we investigated the influence of different substituents on both aromatic rings of the chalcone scaffold on the viability of eight human leukaemia cell lines.

The aim of this study was (i) to synthesize a collection of chalcone derivatives characterized by the presence of a 2'-hydroxy and the presence/absence of a benzyloxy group on the A ring and the presence of halogens (F, Cl, Br, CF<sub>3</sub>, two atoms of fluoride, a methoxy and a fluoride), a methoxy, one or two benzyloxy radicals, a morpholinyl and a 2-pyridyl on the B ring and, (ii) to determine their effects on cell viability in eight human leukaemia cells. We also investigated the signal transduction pathways of cell death induced by 6'-benzyloxy-2'-hydroxy-4-(2-pyridyl)-chalcone (BHP), the most potent viability inhibitor against human leukaemia cells in this group. U-937 and HL-60 cells are often used in biomedical research to determine the cytotoxic potency of compounds with potential therapeutic activity and were selected as models [23,24].

## 2. Results

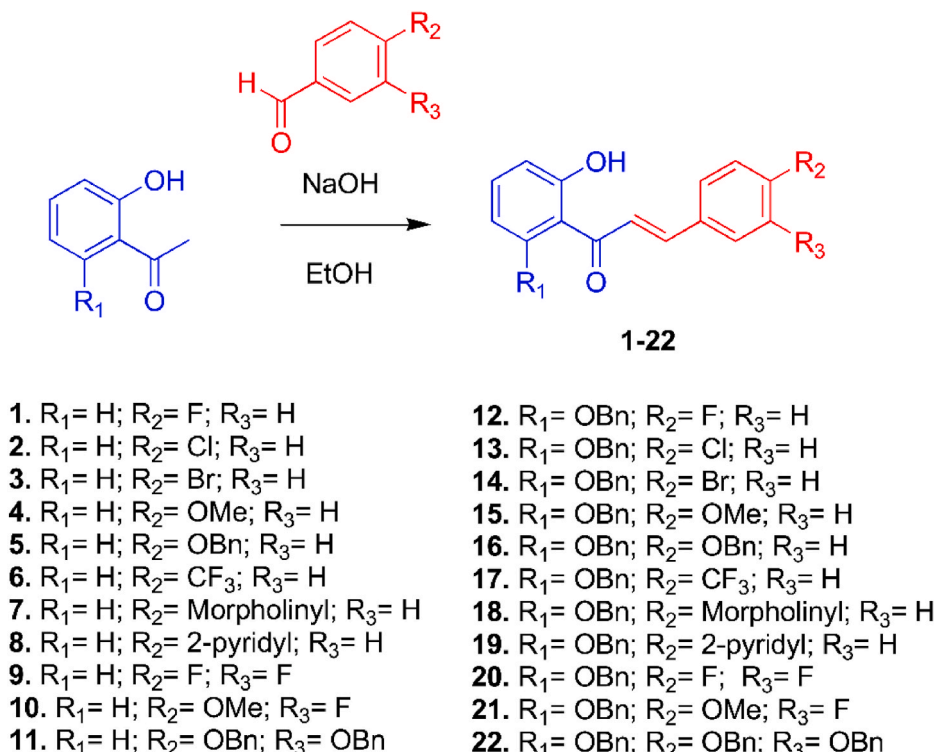
### 2.1. Chemistry

The chalcones (1–22) were prepared following a standard aldol condensation procedure and combining three different benzaldehydes with three different acetophenones (Scheme 1) [25].

### 2.2. Biology

#### 2.2.1. Screening of synthetic chalcones reveals that 6'-benzyloxy-2'-hydroxy-4-(2-pyridyl)-chalcone (BHP) is the most potent inhibitor of viability of human leukaemia cells

The structure–activity relationships (SARs) of a series of chalcones were investigated for their ability to inhibit the viability of human leukaemia cells. These compounds were characterized for the absence or the presence of a benzyloxy radical on the A ring and different substitutions on the B ring of the chalcone scaffold (Scheme 1). Human leukaemia cells used in this study were U-937 (pro-monocytic, human myeloid leukaemia), U-937/Bcl-2 (a cell line overexpressing human Bcl-2), HL-60 (acute myeloid leukaemia), K-562 (chronic myeloid leukaemia), K-562/ADR (a cell line resistant to doxorubicin), MOLT-3



Scheme 1. Synthesis of chalcones.

(acute lymphoblastic leukaemia), JURKAT (acute lymphoblastic leukaemia) and NALM-6 (human B cell precursor leukaemia). To evaluate the effects of chalcones on viability, cells were incubated with increasing concentrations of each compound for 72 h and the IC<sub>50</sub> values (the concentrations that induce a 50 % inhibition of viability) determined by the MTT colorimetric method (Table 1).

These results revealed the following. In the case of chalcones containing only an atom of halogen at position 4 on the B ring (chalcones 1, 2 and 3), the 2'-hydroxychalcones containing a bromine or fluorine atom were the most potent inhibitors of viability and the order of potency was Br ~ F > Cl in four human leukaemia cells, except for U-937, U-937/Bcl-2, JURKAT and NALM-6 cells. In U-937 cells, the monohalogenated compounds were almost equally potent, while in U-937/Bcl-2, JURKAT and NALM-6 the order of potency was Br ~ Cl > F. Substitution of a Br or a F by a Cl led to a significant increase in the IC<sub>50</sub> values in HL-60, K-562, K-562/ADR and MOLT-3. These differences in the IC<sub>50</sub> values of halogenated chalcones were minimized by the introduction of a benzyloxy group at position 6' on the A ring. Chalcones 12, 13 and 14 containing a fluorine, a chlorine and a bromine, respectively, show a similar cell viability inhibition in the leukaemia cells assayed, except in NALM-6, whose IC<sub>50</sub> values were >10 µM.

The results shown here emphasize the importance of the bromine atom in monohalogenated 2'-hydroxychalcones and the benzyloxy group in determining cell viability inhibition independent of the type of halogen.

Substitution of a F or a Br (chalcones 1 and 3) for a methoxy group (chalcone 4) implicated a decrease in the inhibition of cell viability except in HL-60. A similar and even greater decrease in cell viability inhibition was observed following substitution of the methoxy group (chalcone 4) for a benzyloxy group (chalcone 5). The trifluoromethyl derivative (chalcone 6) displayed similar IC<sub>50</sub> values to those of the chlorine derivative (chalcone 2). In general, the IC<sub>50</sub> values for chalcone 6 were >10 µM, except for U-937 cells (IC<sub>50</sub> = 4.6 ± 1.5 µM).

Substitution of the atom of Br (chalcone 3) by a morpholinyl (chalcone 7), a 2-pyridyl (chalcone 8), two atoms of fluorine (chalcone 9), a fluorine and a methoxy (chalcone 10) or two benzyloxy radicals (chalcone 11) on the B ring in 2'-hydroxychalcones did not amplify the inhibition of cell viability. Although substitution of a benzyloxy group (chalcone 5) by a 2-pyridyl (chalcone 8) increased cytotoxicity in all cell lines assayed, the presence of two atoms of fluorine (chalcone 9) or the pair 3-F, 4-MeO- (chalcone 10) did not enhance cytotoxicity relative to the fluorochalcone (chalcone 1). The only exception was in U-937 and MOLT-3, whose IC<sub>50</sub> values were lower in chalcone 9 (containing two atoms of fluorine in *ortho* position on the B ring) than chalcone 1 (containing an atom of fluorine in *para* position on the B ring).

The presence of a methoxy (chalcone 15), a benzyloxy (chalcone 16) or a morpholinyl (chalcone 18) group instead of halogen did not affect inhibition of viability. Surprisingly, the trifluoromethyl derivative (chalcone 17) retained the same capacity of viability inhibition as the monohalogenated chalcones containing a benzyloxy radical (12, 13 and 14) in HL-60, K-562, K-562/ADR, MOLT-3, JURKAT and NALM-6.

Chalcone 19, BHP, containing a pyridine ring and a benzyloxy radical was the most potent inhibitor of viability and showed IC<sub>50</sub> values that were lower than those for monohalogenated chalcones containing a benzyloxy radical in the eight human leukaemia cell lines.

The last three compounds of this series contained two substituents in *ortho* positions on the B ring: two atoms of fluorine (chalcone 20), a fluorine and a methoxy group (chalcone 21) and two benzyloxy radicals (chalcone 22). Chalcone 20 displayed very similar IC<sub>50</sub> values to the corresponding monofluorine chalcone (chalcone 12), except for JURKAT and NALM-6. However, substitution of the fluorine at position 4 on the B ring (chalcone 20) by a methoxy group (chalcone 21) decreased the activity in the majority of cell lines, but not in JURKAT and NALM-6. Chalcone 22 exhibited very low cytotoxicity against the leukaemia cells assayed, probably due to low solubility originating from the presence of the three benzyloxy groups. In these experiments,

etoposide, an antineoplastic agent and topoisomerase II poison, was included as a positive control.

These results suggest that the main determinant of viability inhibition in this series of chalcones is the presence of a benzyloxy radical on the A ring, one or two halogens in *ortho* position or a heterocycle of pyridine on the B ring, and that BHP was the most potent inhibitor in all human leukaemia cell lines assayed (Table 1).

The SAR of chalcone analogues is shown in Fig. 1. In summary, inhibition of cell viability was enhanced by (i) the presence of a benzyloxy group on the A ring, (ii) one halogen atom or two fluorine atoms on the B ring, and (iii) the combination of a benzyloxy group on the A ring with a 2-pyridyl substituent at position 4 on the B ring, which yielded the most potent compound in the series.

Since cell viability inhibition assays revealed that BHP was the most potent inhibitor, it was selected for additional experiments using U-937 and HL-60 cells as models. Fig. 2a represents an example dose-response curve for the inhibition of viability. Phase-contrast microscopy images revealed that BHP caused an important decrease in the number of cells and induced significant morphological changes (Fig. 2b). U-937 cells were more sensitive to the effects on viability of BHP than human peripheral blood mononuclear cells obtained from healthy donors (Fig. 2c). These results indicate that BHP inhibited the viability of leukaemia cells while normal quiescent lymphocytes showed no appreciable toxicity even after exposure to 30 µM of chalcone for 24 h.

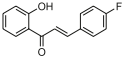
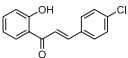
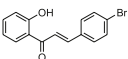
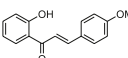
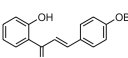
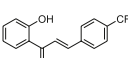
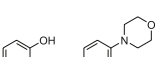

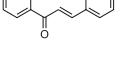
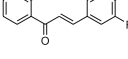
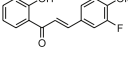
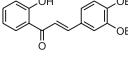
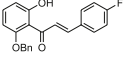
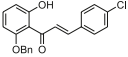
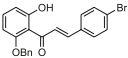
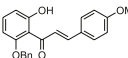
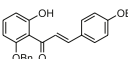
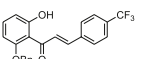
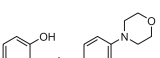
#### 2.2.2. BHP induced apoptosis in human myeloid leukaemia cells

Flow cytometric analyses were performed to determine whether the reduced viability induced by BHP was caused by apoptosis induction. To this end, U-937 cells were treated with BHP (10 µM) for different times (6–24 h) and analyzed by flow cytometry after staining with propidium iodide. As shown in Fig. 3a, BHP was able to induce a seven-fold increase in the percentage of sub-G<sub>1</sub> cells (2.8 % vs. 19.1 %) after 24 h of treatment and this increase in the percentage of sub-G<sub>1</sub> cells was time-dependent (Fig. 3b). A similar trend was observed in HL-60 cells (Supplementary material, Fig. A.1a). The quantification of cell death obtained by measurement of the percentages of sub-G<sub>1</sub> cells by flow cytometry reveals that maximum levels of apoptosis induction were obtained after treatment for 24 h in both cell lines (Fig. 3b and Fig. A.1b). In accordance with the experiments of flow cytometry, nuclei of U-937 and HL-60 cells incubated with 10 µM of BHP for 24 h displayed condensation and fragmentation of chromatin and appearance of apoptotic bodies (Fig. 3c and Fig. A.1c). BHP-induced apoptotic cell death was also assayed and assessed using propidium iodide and annexin V-FITC staining in U-937 and HL-60 cells (Fig. 3d and Fig. A.1d). The percentage of apoptotic cells, determined by the flow cytometric annexin V-FITC assay (Fig. 3d), increased 6.3-fold in U-937 cells treated with BHP for 24 h, and 3.6 times in HL-60 cells (Fig. A.1d). These results indicate that BHP induces apoptosis in human myeloid leukaemia cell lines U-937 and HL-60.

#### 2.2.3. BHP induced caspase activation and poly(ADP-ribose) polymerase cleavage

To determine whether BHP is able to induce poly(ADP-ribose) polymerase (PARP) cleavage, considered to be a hallmark of apoptosis and indicative of caspase activation, nuclear fractions of treated cells for different time periods were analyzed by immunoblotting. As shown in Fig. 4a, BHP induced PARP cleavage into a 85 kDa fragment generated from the full-length PARP protein after 6 h exposure at a concentration of 10 µM. Processing of caspases in cells treated with BHP was also analyzed by immunoblotting to determine the temporal relationship between caspase activation and PARP cleavage. Executioner caspase-3 was processed, as detected by a decrease in the proenzyme. Initiator caspases were also processed: procaspase-9 and procaspase-8 showed reduced levels of their respective proenzymes starting at 6 h in U-937 cells (Fig. 4a), whereas in HL-60 cells, a decrease in procaspase-8 was observed after 12 h of treatment (Fig. A.2a). The levels of cleaved

**Table 1**  
Effects on viability of synthetic chalcones on human leukaemia cells.

Compound		IC <sub>50</sub> (μM)							
		U-937	U-937/Bcl-2	HL-60	K-562	K-562/ADR	MOLT-3	JURKAT	NALM-6
1		8.5 ± 1.2	15.6 ± 3.8	10.5 ± 1.5	13.9 ± 0.7	14.5 ± 3.1	8.0 ± 0.8	24.0 ± 1.0	33.4 ± 5.2
2		4.5 ± 1.8	9.0 ± 4.6	28.5 ± 0.7	28.0 ± 1.4	25.5 ± 0.9	16.3 ± 2.0	9.3 ± 2.1	9.1 ± 3.2
3		5.6 ± 1.0	6.2 ± 0.9	7.9 ± 0.8	10.9 ± 1.8	7.4 ± 2.0	7.7 ± 1.9	9.5 ± 1.6	8.5 ± 3.1
4		21 ± 1.4	21.1 ± 3.5	7.5 ± 0.9	19.9 ± 1.3	24.9 ± 1.2	12.7 ± 0.9	42.4 ± 12.7	42.7 ± 6.9
5		23.7 ± 0.8	28.8 ± 6.4	21.4 ± 4.0	43.0 ± 4.2	28.4 ± 1.5	20.3 ± 0.6	38.6 ± 2.2	46.3 ± 6.0
6		4.6 ± 1.5	15.0 ± 2.4	14.9 ± 6.8	25.5 ± 4.9	28.0 ± 3.0	15.4 ± 0.1	19.4 ± 4.3	16.6 ± 2.5
7		26.8 ± 2.8	23.5 ± 6.0	25.8 ± 0.3	29.8 ± 1.7	30.6 ± 3.7	23.8 ± 0.9	>100	>100
8		10.3 ± 4.0	22.2 ± 4.7	16.8 ± 1.6	19.5 ± 0.7	23.1 ± 2.2	10.7 ± 2.2	23.2 ± 7.2	36.5 ± 3.8
9		4.7 ± 2.2	22 ± 3.2	27.1 ± 8.3	25.0 ± 3.0	20.0 ± 1.0	3.4 ± 0.1	25.5 ± 9.2	40.1 ± 2.6
10		8.2 ± 0.6	12.3 ± 2.4	7.5 ± 0.8	17.0 ± 0.5	12.1 ± 2.7	5.8 ± 0.7	21.1 ± 6.6	27.5 ± 6.0
11		41.2 ± 24.6	63.8 ± 7.4	>100	76.0 ± 28.3	79.0 ± 25.5	22.3 ± 3.8	33.4 ± 16.9	>100
12		6.9 ± 1.2	4.9 ± 1.7	6.1 ± 1.1	4.8 ± 0.1	9.1 ± 3.2	4.5 ± 1.5	8.1 ± 2.4	14.7 ± 3.3
13		4.7 ± 3.0	4.7 ± 3.3	5.6 ± 0.7	4.8 ± 0.4	7.8 ± 3.3	5.1 ± 0.2	6.8 ± 1.5	16.0 ± 4.3
14		4.4 ± 1.1	5.0 ± 0.2	4.9 ± 0.5	7.2 ± 0.8	8.9 ± 1.8	4.3 ± 0.4	6.9 ± 1.2	12.3 ± 4.0
15		22.2 ± 4.7	>100	>100	18.3 ± 7.5	38.6 ± 7.7	9.2 ± 1.0	>100	>100
16		>100	>100	>100	>100	>100	>100	>100	>100
17		30.1 ± 2.4	30.0 ± 4.3	6.8 ± 0.1	5.4 ± 0.1	10.8 ± 4.7	5.9 ± 3.2	6.9 ± 1.0	11.8 ± 1.2
18		>100	>100	>100	>100	>100	>100	>100	>100
19		3.4 ± 0.5	2.2 ± 1.2	3.4 ± 0.8	4.1 ± 0.8	4.8 ± 2.3	6.7 ± 0.8	5.3 ± 0.8	4.9 ± 0.7

(continued on next page)

Table 1 (continued)

Compound	IC <sub>50</sub> (μM)							
	U-937	U-937/Bcl-2	HL-60	K-562	K-562/ADR	MOLT-3	JURKAT	NALM-6
<b>20</b>	4.8 ± 1.8	9.4 ± 2.1	3.6 ± 0.3	5.3 ± 0.7	3.9 ± 0.6	3.5 ± 0.6	33.2 ± 9.7	34.5 ± 5.9
<b>21</b>	14.2 ± 5.2	54.9 ± 5.4	8.7 ± 0.5	18.6 ± 4.9	7.6 ± 1.1	12.9 ± 1.5	13.8 ± 4.1	17.0 ± 2.0
<b>22</b>	>100	>100	>100	>100	>100	>100	>100	>100
<b>Etoposide</b>	1.2 ± 0.3	0.6 ± 0.4	0.4 ± 0.1	0.6 ± 0.1	54 ± 2.8	0.2 ± 0.1	23.3 ± 3.8	4.1 ± 0.8

Cells were cultured for 72 h and the IC<sub>50</sub> values were determined as described in the Material and methods Section. Data are expressed as means ± SEM from the dose-response curves of 3–5 independent experiments with three determinations in each.

**Benzyloxy group enhances the activity**

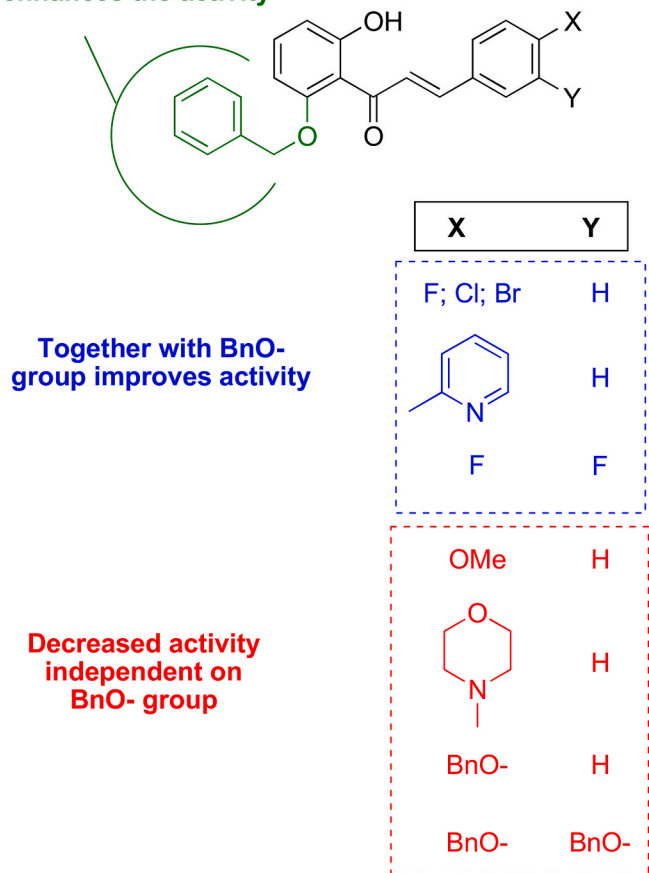


Fig. 1. Structure-activity relationship of chalcone analogues.

caspase-3 peaked at 12 h coinciding with the peak of cleaved caspase-8 (Fig. 4a). These processing patterns in U-937 cells suggest that the early PARP cleavage before caspase-3 processing might be due to caspase-9/caspase-7 cleavage, and then caspase-3 activation could enhance PARP hydrolysis. In HL-60 cells the processing of procaspase-3 and procaspase-9 were detected at 6 h of treatment suggesting that caspase-3 might be involved in PARP cleavage (Fig. A.2a). Caspase-3 processing was also done together with etoposide (3 μM) as a positive control in both U-937 (Fig. 4b) and HL-60 cells (Fig. A.2b).

To investigate whether caspase activation is associated in the mechanism of cell death triggered by BHP in human leukaemia cells, the enzyme activity of cell lysates on specific tetrapeptide substrates was

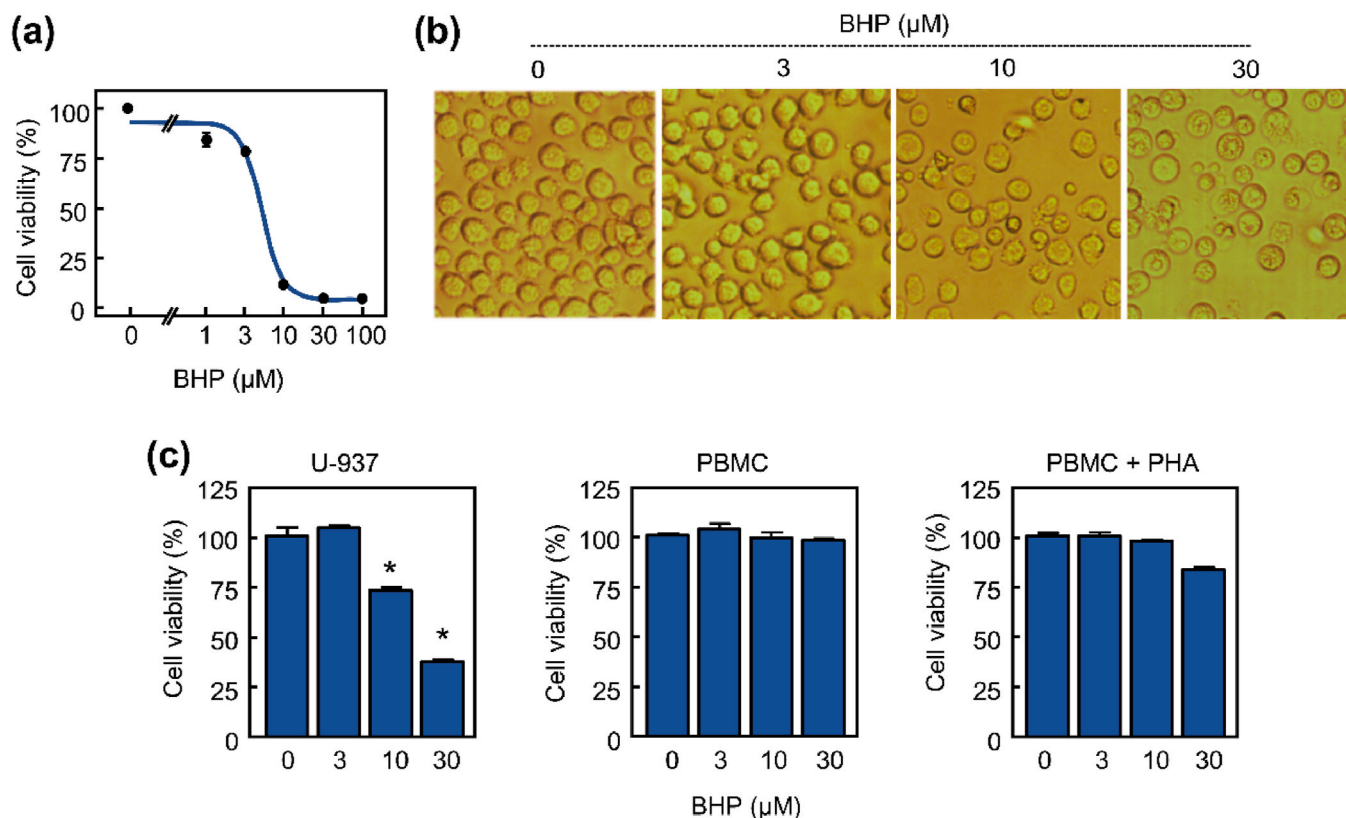
determined after treatment with 10 μM compound for 24 h. As shown in Fig. 4c and Fig. A.2c, caspase-3/7, -8 and -9 activities were detected in U-937 and HL-60 cells. In the caspase-3/7 activation assays, etoposide was included as a positive control in both U-937 (Fig. 4c) and HL-60 cells (Fig. A.2c). To confirm that caspase activation plays a key role in the mechanism of regulated cell death, additional experiments were performed using general and specific caspase inhibitors. Cells were pre-treated with 100 μM z-VAD-fmk and then exposed to BHP for 24 h, followed by flow cytometry analysis. The results showed that the pan-caspase inhibitor led to sub-G<sub>1</sub> cells being almost completely lost (Fig. 4c and Fig. A.2c). The experiments with specific inhibitors also revealed that inhibitors for caspase-3/7 and caspase-8 decreased apoptotic cells and the most potent was the caspase-9 inhibitor, indicating that this initiator caspase plays a main role in the mechanism of action at least in U-937 cells.

#### 2.2.4. BHP induced the release of cytochrome c and a decrease in the mitochondrial membrane potential

The release of cytochrome c from the mitochondrial intermembrane space to cytosol initiates caspase-9 activation. Cells were treated for different periods of time and cytosolic fractions were analyzed by western blotting to determine whether BHP induced cell death involves cytochrome c release. As shown in Fig. 5a and Fig. A.2a, cytochrome c release to the cytosol was detected after 6 h of treatment with BHP (10 μM) in U-937 and HL-60 cells. To investigate whether a dissipation of the mitochondrial membrane potential (ΔΨ<sub>m</sub>) was associated with cytochrome c release, cells were treated with vehicle (DMSO) or BHP for 6 h and 12 h, and analyzed by flow cytometry after staining with the fluorochrome JC-1. The results showed that ΔΨ<sub>m</sub> decreased after 6 h of treatment, suggesting that the reduction of the mitochondrial membrane potential was implicated in BHP-induced cell death (Fig. 5b and c and Fig. A.2d).

Inhibition experiments with the specific caspase-9 inhibitor revealed that the intrinsic pathway plays a key role in the mechanism of BHP-induced cell death. However, the over-expression of Bcl-2 did not block the inhibition of cell viability triggered by BHP in U-937/Bcl-2 cells as indicated above in Table 1. To determine whether the inhibition of viability initiated by BHP was associated with changes in the expression of the Bcl-2 family proteins, cells were incubated with increasing concentrations of BHP for 24 h and whole cell lysates were analyzed by western blotting. As shown in Fig. A.3, changes in the expression of the survival protein Bcl-2 or in the levels of the pro-apoptotic Bax were not observed, at least for U-937 cells. The expression of death receptor 4 (DR4), which is implicated in the extrinsic pathway of cell death, was also explored. As shown in Fig. A.3, BHP failed to affect the expression levels of DR4, also for U-937 cells.





**Fig. 2. BHP inhibited viability of human U-937 cells.** (a) Cells were incubated with increasing concentrations of BHP for 72 h and viability was determined by the MTT assay. (b) Phase-contrast microscopy images of cells treated with the indicated concentrations of BHP for 24 h; original magnification 20x. (c) Differential effect of BHP on viability of U-937 vs. normal peripheral blood mononuclear cells (PBMC) and phytohemagglutinine (PHA, 2  $\mu\text{g}/\text{mL}$ )-activated human PBMC. Cells were incubated with the indicated concentrations of BHP for 24 h and viability was determined by the MTT assay. Bars represent means  $\pm$  SEs of three independent experiments each performed in triplicate. \*Significant difference from the untreated control ( $P < 0.05$ ).

#### 2.2.5. BHP increased production of reactive oxygen species and cell death was decreased by *N*-acetyl-L-cysteine and reduced L-glutathione

An increase in reactive oxygen species (ROS) may induce death in leukaemia cells [26]. To explore whether BHP induces ROS, cells were treated with BHP, stained with the fluorescent probe 2',7'-dichlorodihydrofluorescein diacetate ( $\text{H}_2\text{DCF-DA}$ ) and analyzed by flow cytometry. BHP induced an increase in DCF fluorescence in U-937 and HL-60 treated cells as detected by a rightward shift in fluorescence, but not in PBMC (Fig. 6a and Fig. A.2f and A.2g). To investigate whether oxidative stress triggered by BHP is essential for cell death, U-937 cells were pre-treated with *N*-acetyl-L-cysteine (NAC, 5 mM) or reduced L-glutathione (GSH, 5 mM). As shown, these antioxidants were able to reduce the increase in the percentage of sub-G<sub>1</sub> cells and ROS generation (Fig. 6b and c).

#### 2.2.6. BHP activated the MAPK pathway and cell death was partially blocked by the specific inhibitor of $\text{p38}^{\text{MAPK}}$

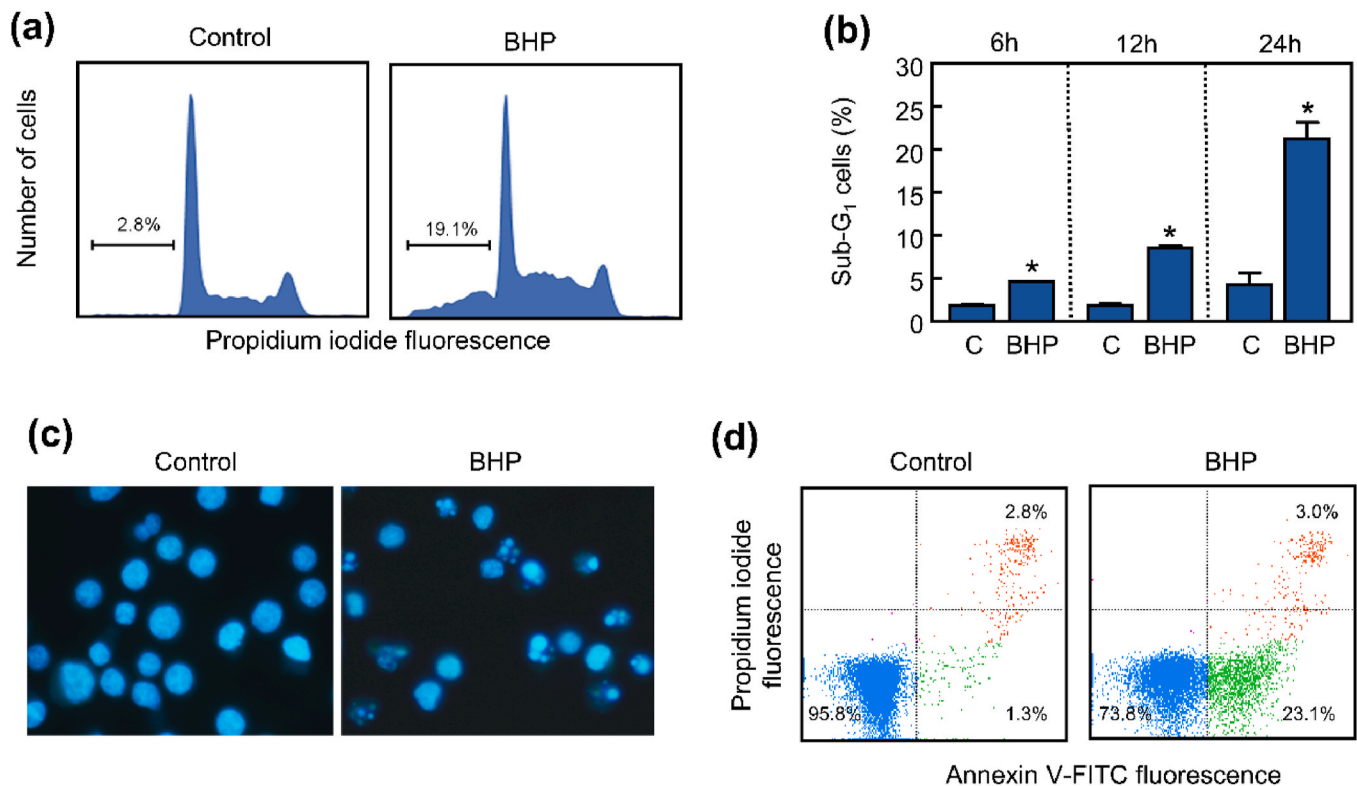
Since ROS can activate the mitogen-activated protein kinase (MAPK) cascade [26–29], the possibility that BHP was able to activate this pathway was also examined. As shown (Fig. 7a), BHP led to phosphorylation of  $\text{p38}^{\text{MAPK}}$ , extracellular signal-regulated kinases 1/2 (ERK1/2) and c-jun N-terminal kinases/stress-activated protein kinases (JNK/SAPK) in U-937 cells. To investigate whether phosphorylation of MAPKs plays a key role in the mechanism of regulated cell death triggered by BHP, additional experiments were done using specific inhibitors. Inhibition of the  $\text{p38}^{\text{MAPK}}$  using SB203580 led to a 35.3 % decrease in BHP-induced cell death. In contrast, the mitogen-activated extracellular kinases 1/2 (MEK1/2) inhibitors, PD98059 and U0126, did not affect BHP-induced cell death. However, a small increase in the percentage of sub-G<sub>1</sub> cells was observed with the JNK/SAPK inhibitor,

SP600125, in the combination group (Fig. 7b).

### 3. Discussion

A PubMed search indicated that little is known about chalcone analogues combining halogens or pyridine with a benzyloxy group that selectively inhibit cancer cell viability [30]. Synthetic chalcones with substituted aromatic rings have been previously reported as ATP binding cassette G2 inhibitors [31]. The presence of methoxy groups in cyclized chalcones confers greater potency to inhibition of cancer cell proliferation than their corresponding nonmethoxylated analogues [32]. Cyclized chalcones containing lipophilic moieties and/or methoxy groups are more bioavailable, stable and potent, and have greater effectiveness than those lacking such groups [33–36]. Previous studies on U-937 cells revealed that the 2'-hydroxychalcone derivative containing a bromine atom at *para* position and a benzyloxy at position 6' is a greater inhibitor of cell viability ( $\text{IC}_{50} = 4.4 \mu\text{M}$ ) than the 2'-hydroxychalcone ( $\text{IC}_{50} = 42.0 \mu\text{M}$ ) derivative containing a bromine atom at position 4 ( $\text{IC}_{50} = 17.0 \mu\text{M}$ ). In addition, the 2'-hydroxychalcone containing a benzyloxy group at position 6' shows a similar cell viability inhibition to the derivative containing an additional bromine atom at position 4 ( $\text{IC}_{50} = 5.0 \mu\text{M}$ ) [37].

Here, we found that the introduction of one or two halogens and a heterocycle of pyridine on the B ring together with a benzyloxy group, improved inhibition of human leukaemia cell viability. SAR analysis revealed that the chalcone bearing both a 2-pyridyl group at position 4 on the B ring and a benzyloxy group on the A ring (BHP) was the most potent inhibitor of cell viability across the eight leukaemia cell lines tested. The U-937 cells were more sensitive to this chalcone compared to normal peripheral blood mononuclear cells (PBMC). The  $\text{IC}_{50}$  values



**Fig. 3.** BHP induced regulated cell death by apoptosis in human U-937. (a) Cells were cultured with 10  $\mu$ M BHP for 24 h and cell death was assayed using propidium iodide staining and FACS. Apoptotic cells (sub-G<sub>1</sub> cells) are shown in region marked with a bar. (b) Cells were treated as above for increasing periods of time and the percentage of sub-G<sub>1</sub> was determined as above. Bars represent means  $\pm$  SEs of three independent experiments each performed in triplicate. \* $P < 0.05$ , significantly different from the untreated control. (c) Photomicrographs of representative fields of cells treated as in (a) and nuclear staining was performed with Hoechst 33258 and visualized with a microscope of fluorescence. (d) Cells were treated as in (a), and apoptosis was assayed using Annexin V-FITC/propidium iodide staining and FACS.

were very similar in the cell lines and, in the case of U-937, was  $3.4 \pm 0.5 \mu$ M and therefore similar to the value obtained with the topoisomerase II inhibitor and antineoplastic agent etoposide ( $IC_{50} = 1.2 \pm 0.3 \mu$ M). Moreover, the human leukaemia cell line overexpressing Bcl-2 protein (U-937/Bcl-2) was also sensitive to this chalcone. The  $IC_{50}$  value in U-937/Bcl-2 cells was  $2.2 \pm 1.2 \mu$ M, similar to the value obtained for U-937 cells. This suggests that this compound might inactivate the protection conferred by Bcl-2.

We analyzed the human chronic myelogenous leukaemia K-562 and found that this cell line is also sensitive to BHP. This is noteworthy given that K-562 cells are reported to be highly resistant to apoptosis induced by 1- $\beta$ -D-arabinofuranosylcytosine, etoposide, paclitaxel, and camptothecin [38–42]. Moreover, this chalcone inhibited the K-562/ADR viability while its  $IC_{50}$  value was similar to the value obtained for K-562. This result is also of note because this chalcone might block the multi-drug resistance conferred by P-glycoprotein that is a major limitation of the clinical efficacy of microtubule-targeting agents.

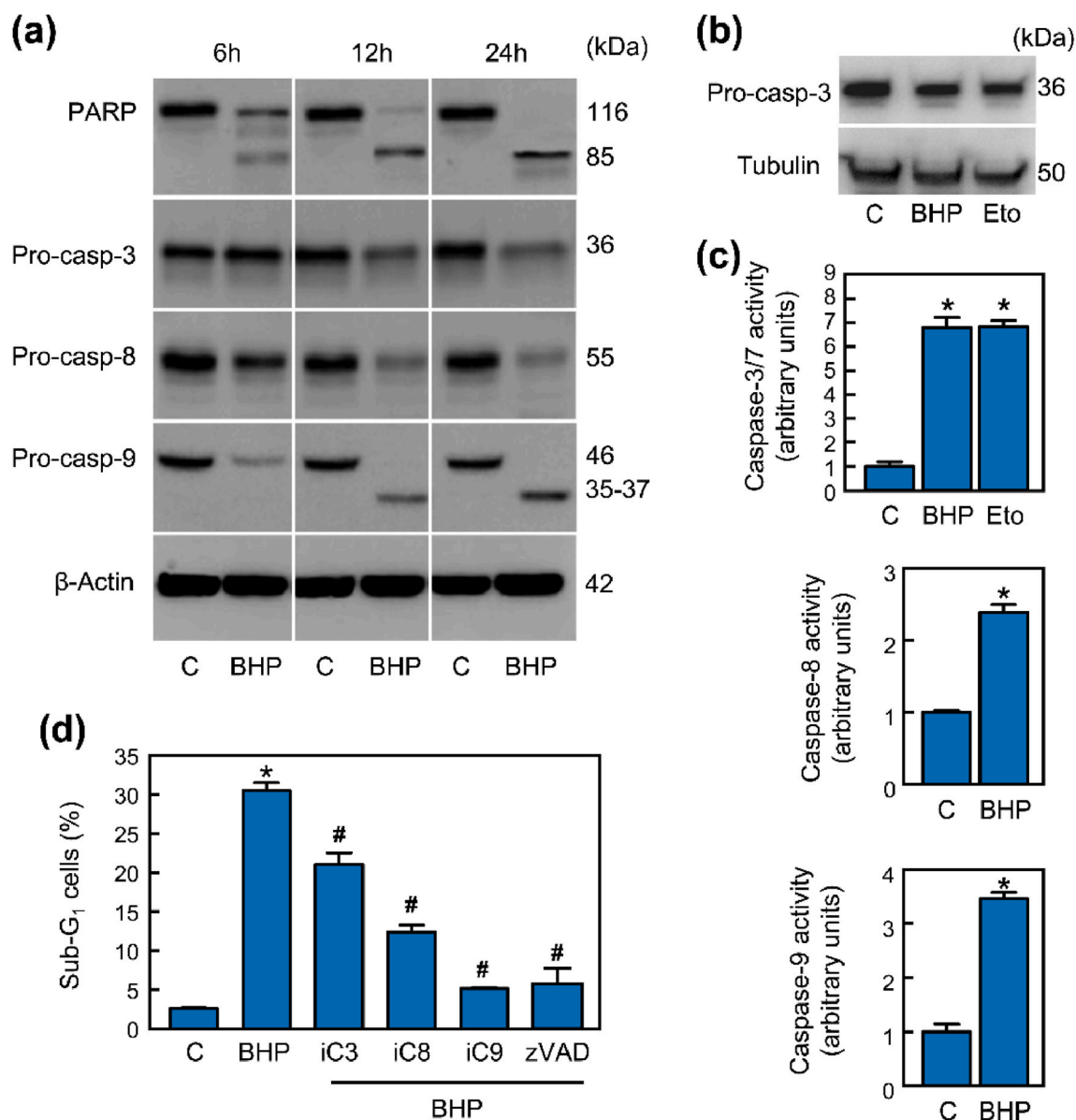
To our knowledge, this is the first time to date that this specific chalcone has been described in relation to its toxic effects on leukaemia cells. Our results show that BHP induced chromatin condensation and fragmentation together with increases in annexin V positive cells and sub-G<sub>1</sub> cells, without causing significant arrest in any phase of the cell cycle. Cell death triggered by this chalcone was associated with the activation and processing of initiator and executioner caspases.

A known substrate for caspase-3/7 like proteases is poly(ADP-ribose) polymerase (PARP) protein that is involved in DNA repair and the cleavage of PARP is a sensitive marker of caspase-mediated apoptosis [43]. The temporal relationship between caspase activation and PARP cleavage after BHP treatment suggests that the early PARP fragmentation might be caused firstly by activation of caspase-9 and then

caspase-3, which might amplify PARP processing. Cell death triggered by BHP was dependent on caspases since (at least in U-937 cells) the pan-caspase inhibitor z-VAD-fmk and also the specific caspase-9 inhibitor z-LEHD-fmk were able to significantly reduce the percentage of sub-G<sub>1</sub> cells. Contrary to expectations, the caspase-3/7 inhibitor only partially reduced BHP-induced cell death. Nevertheless, our results clearly demonstrate that BHP activates caspase-3/7 in a manner similar to etoposide, which served as a positive control for caspase activation. Previous studies have shown that this competitive inhibitor is more effective against caspase-3 than caspase-7 [43]. A plausible explanation for its limited effect is that other executioner caspases, such as caspase-7 or caspase-6, also contribute to BHP-induced cell death. BHP induced an early release of cytochrome c which was accompanied by mitochondrial transmembrane potential dissipation. Collectively, the results highlight that the intrinsic pathway is a major contributor to the mechanism of cell death.

Overexpression of the anti-apoptotic protein Bcl-2 did not block the inhibition of cell viability suggesting that this protein might be a potential target in the mechanism of cell death. Moreover, this chalcone failed to down-regulate the Bcl-2 protein nor did it increase Bax levels after 24 h of treatment. The lack of protection of Bcl-2 overexpression could be explained by the activation of the extrinsic pathway or inactivation of Bcl-2. Cell death induction in leukemic cells overexpressing Bcl-2 might have clinical potential since elevated anti-apoptotic Bcl-2 is associated with chemoresistance in hematological cancers [44]. Future studies will be needed to determine the involvement of additional Bcl-2 members in the mechanism of cell death.

ROS generation is a key trigger of oxidative stress and cell death [45]. Our data show that BHP rapidly elevates ROS in U-937 and HL-60 cells, but not in PBMC, suggesting that the selective sensitivity of



**Fig. 4.** BHP induced caspase activation in human U-937 cells. (a) Time-course of poly(ADP-ribose) polymerase (PARP) cleavage and caspase processing. Cells were treated with 10  $\mu$ M BHP, harvested at indicated times and lysates were analyzed by Western blot.  $\beta$ -Actin was used as a loading control. (b) Immunoblotting for the cleavage of caspase-3 after 24 h incubation with 10  $\mu$ M BHP. Etoposide (Eto, 3  $\mu$ M) was included as a positive control. Tubulin was used as a loading control. (c) Cells were treated with 10  $\mu$ M BHP for 24 h and lysates were assayed for caspase activity using the specific substrates DEVD-pNA, IETD-pNA and LEHD-pNA for caspase-3/7, caspase-8 and caspase-9, respectively. Etoposide (Eto, 3  $\mu$ M) was included as a positive control for caspase-3/7 activation. Results are expressed as fold increases in enzyme activity in comparison with control. Bars represent means  $\pm$  SEs of two independent experiments performed in triplicate. \* $P$  < 0.05 from untreated control. (d) Cells were treated with BHP (10  $\mu$ M, 24 h) in the absence or the presence of the specific caspase inhibitors iC3 (z-DEVD-fmk, 50  $\mu$ M), iC8 (z-IETD-fmk, 50  $\mu$ M), iC9 (z-LEHD-fmk, 50  $\mu$ M) or the pan-caspase inhibitor z-VAD-fmk (100  $\mu$ M) and the percentage of sub-G<sub>1</sub> cells was quantified by flow cytometry after staining with propidium iodide. Bars represent means  $\pm$  SE of two independent experiments performed in duplicate. \*Significant difference from the untreated control ( $P$  < 0.05). #Significant difference from BHP treatment ( $P$  < 0.05).

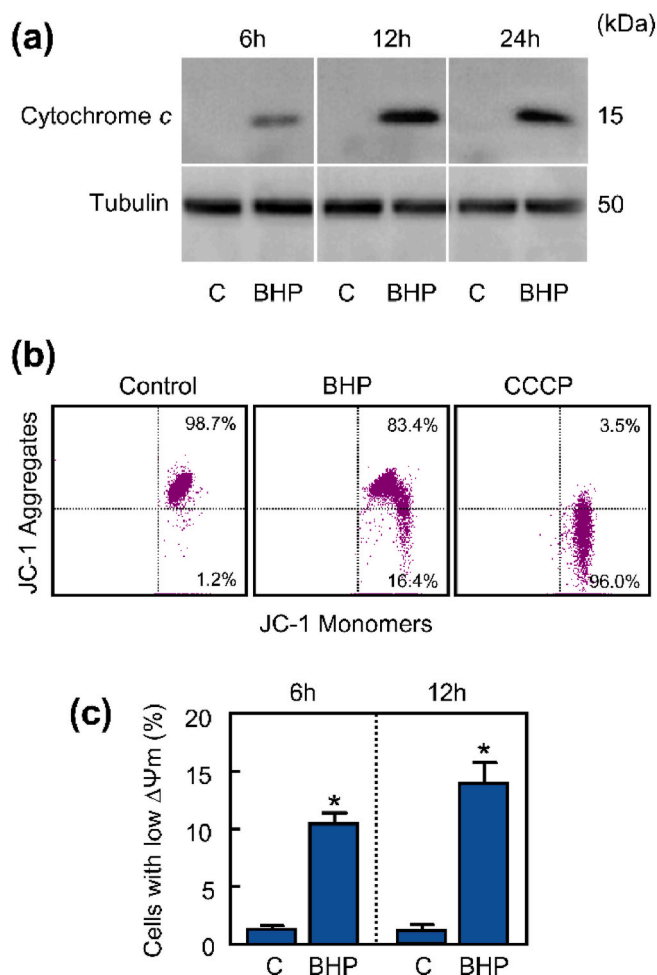
leukaemia cells may relate to their oxidative status. Mitochondrial dysfunction in leukaemia cells—characterized by increased proton leak and reduced coupling efficiency—has been associated with heightened vulnerability to drugs targeting mitochondrial pathways [46]. Future studies should clarify the specific death mechanisms engaged by BHP in malignant versus normal cells. Another noteworthy point is that ROS generation and an increase in sub-G<sub>1</sub> cells was greatly blocked by the antioxidants *N*-acetyl-L-cysteine and glutathione suggesting that oxidative stress is involved in cell death. Furthermore, BHP was able to activate the mitogen-activated protein kinase (MAPK) pathway that is involved in cell proliferation, survival and death [47]. Specifically, BHP induced phosphorylation and activation of p38<sup>MAPK</sup>, ERK1/2 and

JNK/SAPK and inhibition of p38<sup>MAPK</sup> led to a partially reduction of cell death.

#### 4. Conclusions

In summary, we synthesized a series of chalcones with or without a benzyloxy group on the A ring and different substituents on the B ring and explored their inhibition of the viability of leukaemia cells. The SARs against leukaemia cells revealed that: (i) the presence of a bromine atom in 4-halogen-chalcone generated a more potent compound than a corresponding 2'-hydroxy group; (ii) the introduction of a benzyloxy radical in position 6' as an ether group enhanced the activity





**Fig. 5.** BHP induced cytochrome *c* release and decreased the mitochondrial membrane potential. (a) Representative immunoblots show the time-dependent cytochrome *c* release by BHP. Cells were cultured with 10  $\mu$ M BHP for the indicated times and cytosolic fractions were obtained and analyzed on Western blots. Tubulin was used as a loading control. (b) Cells were incubated with 10  $\mu$ M BHP for 12 h, and  $\Delta\Psi_m$  was analyzed by flow cytometry after staining with the JC-1 probe. Similar results were obtained in two independent experiments each performed in triplicate. The protonophore carbonyl cyanide *m*-chlorophenylhydrazone (CCCP, 50  $\mu$ M) was used as a positive control. (c) Cells were treated as in (b) for the indicated times, stained with JC-1 and the percentages of cells with reduced  $\Delta\Psi_m$  were quantified by flow cytometry. Bars represent means  $\pm$  SEs of two independent experiments performed in duplicate. \* $P < 0.05$  from untreated control.

independent on the halogen atom; and (iii) the simultaneous presence of a heterocycle of pyridine or two fluorine atoms in an *ortho* position on the B ring and a radical benzyloxy at 6' position on the A ring amplified the cytotoxicity. The 4-(2-pyridyl)-chalcone containing a benzyloxy group at 6' on the A ring (BHP) was the most potent cytotoxic compound tested against the eight human leukaemia cell lines. BHP showed low cytotoxicity against quiescent and proliferating human peripheral blood mononuclear cells, suggesting that this compound may have therapeutic potential. Flow cytometry experiments showed that this chalcone induced cell death rather than arresting the cells in any specific phase of the cell cycle. BHP-induced cell death was associated with caspase activation, PARP cleavage, mitochondrial cytochrome *c* release to cytosol, reactive oxygen species generation and activation of the MAPK pathway.

## 5. Material and methods

### 5.1. General method and reagents

Column chromatography was carried out on silica gel 60 (Merck 230–400 mesh) and analytical thin layer chromatography was performed using silica gel aluminum sheets.  $^1\text{H}$  and  $^{13}\text{C}$  NMR spectra were recorded on a Bruker Ascen 400 spectrometer model with standard pulse sequences operating at 400 MHz in  $^1\text{H}$  and 101 MHz in  $^{13}\text{C}$  NMR. Chemical shifts ( $\delta$ ) are given in ppm upfield from tetramethylsilane as internal standard, and the spectra were recorded in appropriate deuterated solvents, as indicated. Coupling constants (*J*) are reported in hertz. EIMS and HREIMS were recorded on a Micromass model Autospec (70 eV) spectrometer. The general inhibitor of caspases z-VAD-fmk [#627610, benzyloxycarbonyl-Val-Ala-Asp(OMe) fluoromethyl ketone] was from Calbiochem (Darmstadt, Germany). The inhibitors z-DEVD-fmk [#550378, benzyloxycarbonyl-Asp(OMe)-Glu(OMe)-Val-Asp(OMe) fluoromethyl ketone], z-IETD-fmk [#550380, benzyloxycarbonyl-Ile-Glu-Thr-Asp(OMe) fluoromethyl ketone], and z-LEHD-fmk [#550381, benzyloxycarbonyl-Leu-Glu-His-Asp(OMe) fluoromethyl ketone] were purchased from BD Pharmingen (San Diego, CA, USA). The inhibitors U0126 (#1144), PD98059 (#1213), SP600125 (#1496), and SB203580 (#1202) were purchased from Tocris (Bristol, UK). Ammonium persulfate (#161-0700), acrylamide, bisacrylamide (#1610146 40 % acrylamide/Bis solution 29:1) and *N,N,N',N'*-tetramethylethylenediamine (#161-0800) were from Bio-Rad (Hercules, CA, USA). Poly(vinylidene difluoride) membranes (#IPVH00010) and Immobilon Western Chemiluminescent HRP Substrate (#WBKLS0500) were from Millipore (Burlington, MA, USA). All other chemicals were obtained from Sigma (Saint Louis, MO, USA). The primary antibodies used for immunoblots were obtained from the following companies (all at 1:1000 dilution): anti-caspase-3 (#ADI-AAP-113) was from Enzo (Ann Arbor, MI, USA); anti-caspase-9 (#9502), anti-caspase-8 (#9746), anti-Bcl-2 (#4223), anti-Bax (#2772), anti-phospho-JNK/SAPK (phosphor T183 + Y185) (#9251), anti-JNK/SAPK (#9252), anti-phospho-p44/42 MAPK (Erk1/2) (Thr202/Tyr204) (#9101), anti-p44/42 MAP Kinase (ERK1/2) (#9102), anti-phospho-p38<sup>MAPK</sup> (T180/Y182) (#9211), anti-p38<sup>MAPK</sup> (#9212), and anti- $\alpha$ -tubulin (#2125) antibodies from Cell Signaling Technology (Beverly, MA, USA). Anti-PARP [poly(ADP-ribose) polymerase] (#551024) and anti-cytochrome *c* (#556433) were from BD Pharmingen (San Diego, CA, USA); anti-DR4 (ab8414) was from Abcam (Cambridge, UK). Anti- $\beta$ -actin (clone AC-74, #A2228) was from Sigma-Aldrich (Saint Louis, MO, USA); Horseradish peroxidase-conjugated secondary antibodies (#NA9310 and #NA9340) from GE Healthcare (Little Chalfont, UK) were used at 1:10,000 dilution.

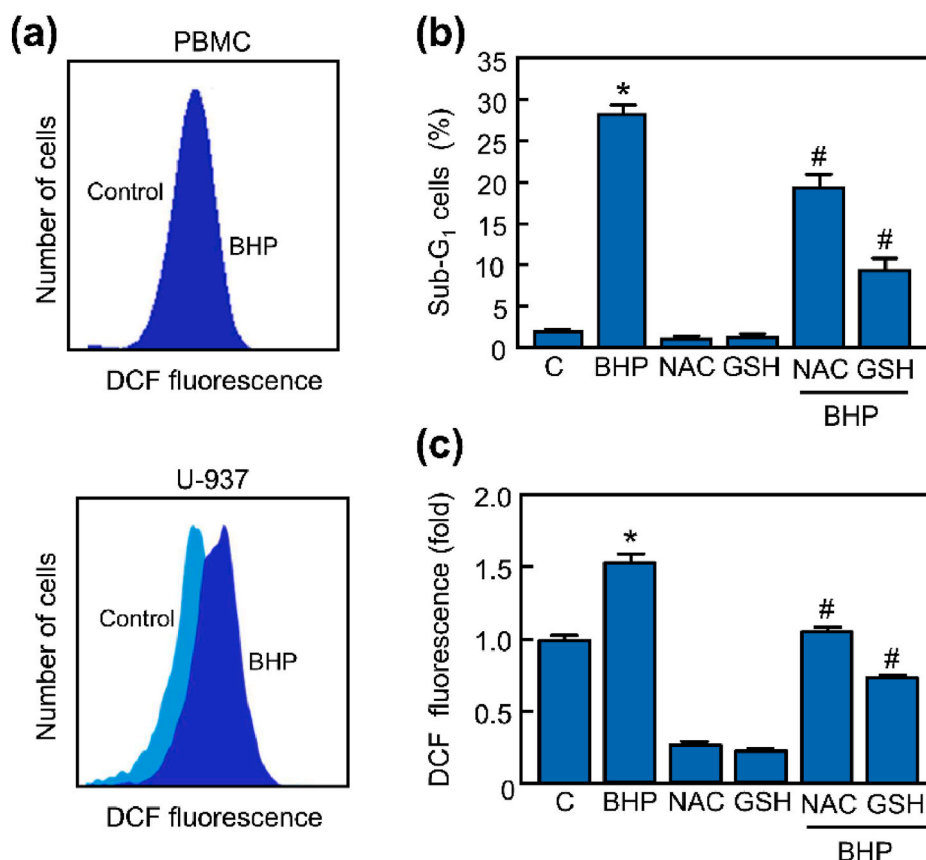
### 5.2. General procedure for the synthesis of chalcones (1–22)

A mixture of the acetophenone (5–10 mmol, 1 equiv) and the corresponding benzaldehyde (1 equiv) in EtOH (20–40 mL) with 50 % aqueous solution of NaOH (5–8 mL) was stirred at room temperature until the starting materials had been consumed. Then HCl (10 %) was added until neutrality. Precipitated chalcones were generally filtered and crystallized from MeOH or purified using column chromatography.

### 5.3. Spectroscopic data of compounds 2, 5, 8–12, 17–22

Spectroscopic data for 1, 3, 4, 6, 7, 13, 15, 14 and 16 have been previously described in Refs. [37,48–54], respectively.

**(E)-1-(2-hydroxyphenyl)-3-(4-(pyridin-2-yl)phenyl)prop-2-en-1-one (8):**  $^1\text{H}$  NMR (400 MHz,  $\text{CDCl}_3$ )  $\delta$  12.82 (s, 1H), 8.78–8.70 (m, 1H), 8.15–8.06 (m, 2H), 8.03–7.97 (m, 1H), 7.96 (d,  $J = 2.1$  Hz, 1H), 7.84–7.76 (m, 4H), 7.73 (d,  $J = 15.4$  Hz, 1H), 7.52 (ddd,  $J = 8.6, 7.1, 1.6$  Hz, 1H), 7.32–7.27 (m, 1H), 7.05 (d,  $J = 8.4$  Hz, 1H), 7.01–6.92 (m, 1H).  $^{13}\text{C}$  NMR (101 MHz,  $\text{CDCl}_3$ )  $\delta$  193.65, 163.65, 156.08, 149.60, 144.77, 141.2, 137.29, 136.50, 135.28, 129.71, 129.19, 127.55, 122.81, 120.91,



**Fig. 6.** BHP induces ROS. (a) Representative histograms of fluorescence obtained by flow cytometry after treatment with 10  $\mu$ M BHP for 3 h. (b) U-937 cells were preincubated with *N*-acetyl-L-cysteine (NAC, 5 mM) or reduced L-glutathione (GSH, 5 mM) for 1 h and then treated for 24 h with 10  $\mu$ M BHP and the percentages of sub-G<sub>1</sub> cells were determined by flow cytometry. (c) Cells were pretreated with *N*-acetyl-L-cysteine (NAC, 5 mM) or reduced L-glutathione (GSH, 5 mM) for 1 h and then incubated for 3 h with 10  $\mu$ M BHP and the fluorescence of oxidized H<sub>2</sub>DCF was determined by flow cytometry. \*Significant difference from the untreated control ( $P < 0.05$ ). #Significant difference from BHP treatment ( $P < 0.05$ ).

120.61, 120.06, 118.92, 118.69. HRMS (ESI-FT-ICR)  $m/z$ : 302.118 [M+H]; calcd. for C<sub>20</sub>H<sub>16</sub>NO<sub>2</sub>: 302.1181.

**(E)-3-(3,4-difluorophenyl)-1-(2-hydroxyphenyl)prop-2-en-1-one (9):** <sup>1</sup>H NMR (400 MHz, CDCl<sub>3</sub>)  $\delta$  12.68 (s, 1H), 7.90 (dd,  $J$  = 8.1, 1.6 Hz, 1H), 7.81 (d,  $J$  = 15.5 Hz, 1H), 7.61–7.45 (m, 3H), 7.39 (ddt,  $J$  = 8.1, 3.9, 1.7 Hz, 1H), 7.29–7.18 (m, 3H), 7.04 (dd,  $J$  = 8.4, 1.2 Hz, 1H), 6.96 (ddd,  $J$  = 8.2, 7.2, 1.2 Hz, 1H). <sup>13</sup>C NMR (101 MHz, CDCl<sub>3</sub>)  $\delta$  193.2, 163.6, 136.7, 129.6, 125.60 (dd,  $J$  = 6.6, 3.5 Hz), 121.13 (d,  $J$  = 2.6 Hz), 193.25, 163.67, 142.95, 136.71, 129.61, 125.64 (d,  $J$  = 3.51 Hz), 125.57 (d,  $J$  = 3.61 Hz), 121.13, (d,  $J$  = 2.59 Hz), 119.85, 118.99, 118.77, 118.13, 117.96, 116.78, 116.61. <sup>19</sup>F NMR (377 MHz, CDCl<sub>3</sub>)  $\delta$  –132.93 (d,  $J$  = 20.7 Hz), –136.21 (d,  $J$  = 21.2 Hz). HRMS (ESI-FT-ICR)  $m/z$ : 259.0572 [M – H]; calcd. for C<sub>15</sub>H<sub>9</sub>O<sub>2</sub>F<sub>2</sub>: 259.0571.

**(E)-3-(3-fluoro-4-methoxyphenyl)-1-(2-hydroxyphenyl)prop-2-en-1-one (10):** <sup>1</sup>H NMR (400 MHz, CDCl<sub>3</sub>)  $\delta$  12.82 (s, 1H), 7.91 (dd,  $J$  = 8.1, 1.6 Hz, 1H), 7.84 (d,  $J$  = 15.4 Hz, 1H), 7.56–7.47 (m, 2H), 7.45 (dd,  $J$  = 12.0, 2.1 Hz, 1H), 7.38 (dt,  $J$  = 8.4, 1.7 Hz, 1H), 7.07–6.97 (m, 2H), 6.95 (td,  $J$  = 7.7, 7.2, 1.2 Hz, 1H), 3.95 (s, 3H). <sup>13</sup>C NMR (101 MHz, CDCl<sub>3</sub>)  $\delta$  193.4, 163.6, 153.7, 151.2, 150.1 (d,  $J$  = 11.0 Hz), 144.1 (d,  $J$  = 2.5 Hz), 136.4, 129.5, 127.8 (d,  $J$  = 6.6 Hz), 126.5 (d,  $J$  = 3.2 Hz), 120.0, 118.9, 118.8, 118.6, 114.9 (d,  $J$  = 18.6 Hz), 113.20 (d,  $J$  = 2.1 Hz), 112.4, 56.32. <sup>19</sup>F NMR (376 MHz, CDCl<sub>3</sub>)  $\delta$  –134.35. HRMS (ESI-FT-ICR)  $m/z$ : 271.0768 [M – H]; calcd. for C<sub>16</sub>H<sub>12</sub>O<sub>3</sub>F: 271.0770.

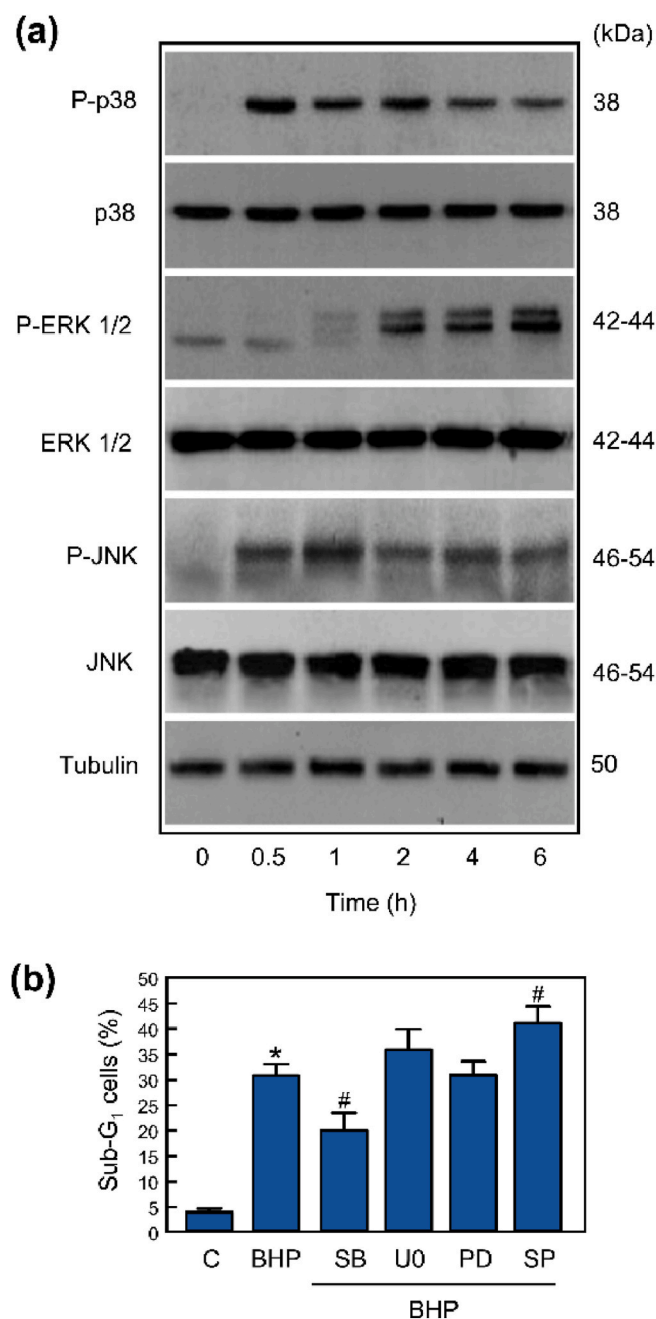
**(E)-1-(2-(benzyloxy)-6-hydroxyphenyl)-3-(4-fluorophenyl)prop-2-en-1-one (12):** <sup>1</sup>H NMR (400 MHz, CDCl<sub>3</sub>)  $\delta$  7.82 (d,  $J$  = 15.6 Hz, 1H), 7.71 (d,  $J$  = 15.6 Hz, 1H), 7.53 (d,  $J$  = 7.3 Hz, 2H), 7.49–7.39 (m, 4H), 7.08 (dd,  $J$  = 8.4, 5.6 Hz, 2H), 6.91 (t,  $J$  = 8.5 Hz, 2H), 6.68 (d,  $J$  = 8.4 Hz, 1H), 6.58 (d,  $J$  = 8.3 Hz, 1H). <sup>13</sup>C NMR (126 MHz, CDCl<sub>3</sub>)  $\delta$

194.34, 165.60, 164.73, 162.74, 160.29, 141.99, 136.15, 135.63, 131.37 (d,  $J$  = 3.2 Hz), 130.35 (d,  $J$  = 8.4 Hz), 128.96, 128.75, 128.64, 127.97, 127.44 (d,  $J$  = 2.4 Hz), 115.81 (d,  $J$  = 21.8 Hz), 102.23, 71.45. <sup>19</sup>F NMR (376 MHz, CDCl<sub>3</sub>)  $\delta$  –109.74. HRMS (ESI-FT-ICR)  $m/z$ : 371.1050 [M – H]; calcd. for C<sub>22</sub>H<sub>17</sub>O<sub>3</sub>FNa: 371.1059.

**(E)-1-(2-(benzyloxy)-6-hydroxyphenyl)-3-(4-(trifluoromethyl)phenyl)prop-2-en-1-one (17):** <sup>1</sup>H NMR (400 MHz, CDCl<sub>3</sub>)  $\delta$  13.36 (s, 1H), 7.88 (d,  $J$  = 15.6 Hz, 1H), 7.67 (d,  $J$  = 15.6 Hz, 1H), 7.52–7.46 (m, 2H), 7.45–7.33 (m, 6H), 7.13 (d,  $J$  = 8.3 Hz, 2H), 6.67 (dd,  $J$  = 8.4, 0.9 Hz, 1H), 6.61–6.50 (m, 1H), 5.12 (s, 2H), 1.55 (s, 1H). <sup>13</sup>C NMR (101 MHz, CDCl<sub>3</sub>)  $\delta$  194.19, 165.59, 160.33, 140.74, 138.67, 136.39, 135.51, 130.21, 128.93, 128.70, 128.34, 125.60, 125.57, 125.53, 125.49, 111.70, 111.50, 102.27, 71.55. HRMS (ESI-FT-ICR)  $m/z$ : 397.1058 [M+Na]; calcd. for C<sub>23</sub>H<sub>16</sub>O<sub>3</sub>F<sub>3</sub>: 397.1052.

**(E)-1-(2-(benzyloxy)-6-hydroxyphenyl)-3-(4-morpholino-phenyl)prop-2-en-1-one (18):** <sup>1</sup>H NMR (400 MHz, CDCl<sub>3</sub>)  $\delta$  13.84–13.43 (m, 1H), 7.86–7.74 (m, 2H), 7.58–7.50 (m, 2H), 7.46–7.35 (m, 4H), 7.12 (d,  $J$  = 8.4 Hz, 2H), 6.73 (d,  $J$  = 8.6 Hz, 2H), 6.67 (d,  $J$  = 8.4 Hz, 1H), 6.55 (d,  $J$  = 8.3 Hz, 1H), 5.16 (s, 2H), 3.93–3.86 (m, 4H), 3.30–3.22 (m, 4H). <sup>13</sup>C NMR (101 MHz, CDCl<sub>3</sub>)  $\delta$  194.18, 165.43, 160.15, 152.49, 143.91, 135.97, 135.46, 130.25, 128.85, 128.38, 128.25, 126.27, 124.28, 114.48, 112.09, 111.41, 102.38, 77.31, 66.65, 48.08. HRMS (ESI-FT-ICR)  $m/z$ : 438.1688 [M+Na]; calcd. for C<sub>26</sub>H<sub>25</sub>NO<sub>4</sub>Na: 438.1681.

**(E)-1-(2-(benzyloxy)-6-hydroxyphenyl)-3-(4-(pyridin-2-yl)phenyl)prop-2-en-1-one (19):** <sup>1</sup>H NMR (400 MHz, CDCl<sub>3</sub>)  $\delta$  13.38 (s, 1H), 8.62 (ddd,  $J$  = 4.8, 1.7, 1.0 Hz, 1H), 7.82 (d,  $J$  = 15.6 Hz, 1H), 7.77–7.73 (m, 2H), 7.71–7.64 (m, 2H), 7.62 (dt,  $J$  = 8.0, 1.2 Hz, 1H),



**Fig. 7. BHP induced MAPK activation.** (a) Representative western blots show the time-dependent phosphorylation of MAPK. Cells were treated with 10  $\mu$ M BHP for the indicated times and MAPK phosphorylation was detected by immunoblotting. Membranes were stripped and reprobed with total ERK, total JNK, total p38<sup>MAPK</sup> and tubulin antibodies as loading controls. (b) Cells were pretreated with SB (SB203580, 2  $\mu$ M), U0126 (UO, 10  $\mu$ M), PD98059 (PD, 10  $\mu$ M) and SP600125 (SP, 10  $\mu$ M) for 1 h and then incubated with 10  $\mu$ M BHP for 24 h and apoptotic cells were quantified by flow cytometry. \* $P < 0.05$  from untreated control. # $P < 0.05$  significantly different from BHP treatment.

7.40 (dd,  $J = 7.6$ , 1.7 Hz, 2H), 7.34–7.26 (m, 4H), 7.15 (ddd,  $J = 7.2$ , 4.9, 1.4 Hz, 1H), 7.12 (d,  $J = 8.3$  Hz, 2H), 6.55 (dd,  $J = 8.4$ , 0.9 Hz, 1H), 6.44 (dd,  $J = 8.3$ , 0.7 Hz, 1H), 5.03 (s, 2H). <sup>13</sup>C NMR (126 MHz, CDCl<sub>3</sub>)  $\delta$  194.41, 165.51, 160.30, 142.70, 136.13, 135.86, 135.60, 129.45, 129.15, 129.03, 129.01, 128.72, 128.66, 128.59, 128.18, 127.31, 127.24, 122.61, 120.85, 111.85, 111.41, 102.32, 71.48. HRMS (ESI-FT-ICR)  $m/z$ : 430.1413 [M+Na]; calcd. for C<sub>27</sub>H<sub>21</sub>NO<sub>3</sub>Na: 430.1419.

**(E)-1-(2-(benzyloxy)-6-hydroxyphenyl)-3-(3,4-difluorophenyl)**

**prop-2-en-1-one (20):** <sup>1</sup>H NMR (400 MHz, CDCl<sub>3</sub>)  $\delta$  13.38 (s, 1H), 7.73 (d,  $J = 15.6$  Hz, 1H), 7.58 (d,  $J = 15.6$  Hz, 1H), 7.48 (dd,  $J = 7.5$ , 2.0 Hz, 2H), 7.45–7.33 (m, 4H), 7.05–6.94 (m, 1H), 6.84 (tq,  $J = 7.5$ , 3.0, 2.6 Hz, 2H), 6.66 (d,  $J = 8.4$  Hz, 1H), 6.55 (d,  $J = 8.2$  Hz, 1H), 5.11 (s, 2H). <sup>13</sup>C NMR (126 MHz, CDCl<sub>3</sub>)  $\delta$  194.1, 165.5, 160.3, 152.3, 151.4, 150.3, 149.3, 140.6, 136.40, 135.44 (d,  $J = 7.4$  Hz), 132.34, 129.05, 129.0, 128.7, 128.6, 125.2, 117.5, 116.3, 111.4, 102.2 (d,  $J = 6.0$  Hz), 71.58. <sup>19</sup>F NMR (376 MHz, CDCl<sub>3</sub>)  $\delta$  -134.44 (d,  $J = 20.7$  Hz), -136.57 (d,  $J = 21.2$  Hz). HRMS (ESI-FT-ICR)  $m/z$ : 365.0990 [M - H]; calcd. for C<sub>22</sub>H<sub>15</sub>F<sub>2</sub>O<sub>3</sub>: 365.0989.

**(E)-1-(2-(benzyloxy)-6-hydroxyphenyl)-3-(3-fluoro-4-methoxyphenyl)prop-2-en-1-one (21):** <sup>1</sup>H NMR (400 MHz, CDCl<sub>3</sub>)  $\delta$  13.50 (s, 1H), 7.73 (d,  $J = 15.5$  Hz, 1H), 7.69–7.60 (m, 1H), 7.49 (dd,  $J = 7.0$ , 2.6 Hz, 2H), 7.44–7.34 (m, 4H), 6.99–6.93 (m, 1H), 6.86–6.74 (m, 2H), 6.65 (dd,  $J = 8.5$ , 1.1 Hz, 1H), 6.55 (dd,  $J = 8.3$ , 1.1 Hz, 1H), 5.12 (s, 2H), 3.91 (s, 3H). <sup>13</sup>C NMR (101 MHz, CDCl<sub>3</sub>)  $\delta$  194.20, 165.50, 160.26, 153.45, 151.00, 149.47 (d,  $J = 11.1$  Hz), 142.20 (d,  $J = 2.5$  Hz), 136.01, 135.52, 128.99, 128.89, 128.47, 126.57, 126.44 (d,  $J = 3.1$  Hz), 114.50 (d,  $J = 18.5$  Hz), 112.86 (d,  $J = 2.1$  Hz), 111.79, 111.41, 102.4, 71.49, 56.24. HRMS (ESI-FT-ICR)  $m/z$ : 401.1172 [M+Na]; calcd. for C<sub>23</sub>H<sub>19</sub>FO<sub>4</sub>Na: 401.1165.

**(E)-1-(2-(benzyloxy)-6-hydroxyphenyl)-3-(3,4-bis(benzyloxy)phenyl)prop-2-en-1-one (22):** <sup>1</sup>H NMR (400 MHz, CDCl<sub>3</sub>)  $\delta$  13.40 (s, 1H), 7.76 (d,  $J = 15.5$  Hz, 1H), 7.70 (d,  $J = 15.5$  Hz, 1H), 7.52–7.19 (m, 19H), 6.96 (d,  $J = 1.9$  Hz, 1H), 6.82–6.70 (m, 2H), 6.70–6.63 (m, 1H), 6.55 (d,  $J = 8.3$  Hz, 1H), 5.23 (s, 2H), 5.16 (s, 2H), 4.96 (s, 2H). <sup>13</sup>C NMR (101 MHz, CDCl<sub>3</sub>)  $\delta$  194.31, 165.17, 160.09, 150.93, 148.76, 143.34, 136.90, 136.87, 135.85, 135.76, 128.85, 128.61, 128.52, 128.33, 127.98, 127.91, 127.82, 127.31, 127.14, 125.94, 122.71, 114.98, 114.43, 112.13, 111.38, 102.53, 71.24, 71.14, 71.01. HRMS (ESI-FT-ICR)  $m/z$ : 565.1990 [M+Na]; calcd. for C<sub>36</sub>H<sub>30</sub>O<sub>5</sub>Na: 565.1991.

#### 5.4. Cell culture

The human leukaemia U-937 (#ACC 5, pro-monocytic, human myeloid leukaemia), HL-60 (#ACC 3, acute myeloid leukaemia), K-562 (#ACC 10, chronic myeloid leukaemia), MOLT-3 (#ACC 84, acute lymphoblastic leukaemia), JURKAT (#ACC 282, acute lymphoblastic leukaemia) and NALM-6 (#ACC 128, human B cell precursor leukaemia) cells were obtained from the German Collection of Microorganisms and Cell Cultures (Braunschweig, Germany). U-937/Bcl-2 cells were provided by Dr. Jacqueline Bréard (INSERM U749, Faculté de Pharmacie Paris-Sud, Châtenay-Malabry, France) and K-562/ADR, a cell line resistant to doxorubicin was provided by Dr. Lisa Oliver (INSERM, Nantes, France). Cells were maintained in a humidified atmosphere at 37 °C with 5 % CO<sub>2</sub> in RPMI 1640 medium supplemented with 10 % (v/v) fetal bovine serum, 2 mM L-glutamine, 100  $\mu$ g/mL streptomycin and 100 U/mL penicillin as described [37]. K-562/ADR cells were cultured in presence of 200 ng/mL doxorubicin. Human peripheral blood mononuclear cells (PBMC) were isolated by centrifugation with Ficoll-Paque Plus (GE Healthcare Bio-Sciences AB, Uppsala, Sweden) from blood anticoagulated with heparin of healthy donors. PBMC were also stimulated with phytohemagglutinine (2  $\mu$ g/mL) for 48 h before the experimental treatment. Viability was always greater than 95 % in all experiments as determined by the trypan blue exclusion method.

#### 5.5. Cell viability assays

Synthetic chalcones were dissolved in DMSO (dimethyl sulfoxide) and kept under dark conditions at -20 °C. Before each experiment, chalcones were dissolved in culture media at 37 °C. The final concentration of DMSO did not exceed 0.3 % (v/v). The effects of chalcones on human leukaemia cell viabilities were evaluated by colorimetric MTT [3-(4,5-dimethyl-2-thiazolyl)-2,5-diphenyl-2H-tetrazolium bromide] assays as described [55]. Cells (5000 per well) were incubated with increasing concentrations of chalcones for 72 h into a 96-well plate.

Supernatants were removed and MTT (0.5 mg/mL) was added and incubated at 37 °C for 4 h and the reaction products were solubilized overnight under dark conditions with sodium dodecyl sulfate (10 % w/v) in 0.05 M HCl. Absorbance was measured at 570 nm using a microplate reader (Bio-Rad, Hercules, CA, USA) and the IC<sub>50</sub> values were determined graphically using nonlinear regression implemented within the curve-fitting routine in the software Prism 5.0 (GraphPad, La Jolla, CA, USA).

#### 5.6. Quantification of apoptosis by fluorescence microscopy and flow cytometry

Fluorescence microscopy experiments were carried out as previously described. Briefly, following BHP treatment, cells ( $7 \times 10^5$ ) were harvested, collected and washed with PBS, fixed in 3 % paraformaldehyde, incubated with Hoechst 33258 (bisbenzimidazole trihydrochloride, 20 µg/mL) and visualized with a Zeiss-Axiovert fluorescence microscope. Flow cytometric analysis using single staining with propidium iodide or double staining with annexin V-fluorescein isothiocyanate and propidium iodide was performed using a BD FACSVerse™ cytometer (BD Biosciences, San Jose, CA, USA) as previously described [37].

#### 5.7. Assay of caspase activity

Caspase activity was measured using specific colorimetric substrates. Briefly, cells were treated with 10 µM BHP for 24 h, harvested by centrifugation (1000×g for 5 min at 4 °C) and homogenized in lysis buffer (50 mM HEPES, pH 7.4, 1 mM dithiothreitol, 0.1 mM EDTA, 0.1 % Chaps), spun (17,000×g for 10 min at 4 °C) and the resulting supernatants normalized by protein concentration were assayed for caspase activity. The net increase in absorbance at 405 nm after incubation at 37 °C was indicative of enzyme activity. The colorimetric substrates were from Calbiochem (Darmstadt, Germany): DEVD-pNA (#235400, N-acetyl-Asp-Glu-Val-Asp-p-nitroaniline), IETD-pNA (#368057, N-acetyl-Ile-Glu-Thr-Asp-p-nitroaniline) and LEHD-pNA (#218805, N-acetyl-Leu-Glu-His-Asp-p-nitroaniline) for caspase-3/7, -8 and -9 activities, respectively.

#### 5.8. Subcellular fractionation and Western blot analysis

Cytosolic fractions and whole cell lysates were subjected to immunoblot analysis as previously described. For subcellular fractionation, harvested cells were washed twice with PBS and then resuspended and incubated on ice for 15 min in lysis buffer [20 mM HEPES (pH 7.5), 1.5 mM MgCl<sub>2</sub>, 10 mM KCl, 1 mM EGTA, 1 mM EDTA, 250 mM sucrose and 1 mM dithiothreitol containing protease inhibitors (0.1 mM phenylmethylsulfonyl fluoride and 1 µg/mL aprotinin, leupeptin and pepstatin A)]. Cells were lysed by pushing them several times through a 22-gauge needle and the lysates were centrifuged at 1,000×g for 5 min at 4 °C. These pellets were used as nuclear fractions. The supernatant fractions were centrifuged at 105,000×g for 45 min at 4 °C, and the resulting supernatants were used as the cytosolic fractions.

For whole cell lysates, cells were washed twice in PBS and pellets were resuspended in lysis buffer [20 mM Tris-HCl (pH 7.4), 137 mM NaCl, 20 mM sodium β-glycerophosphate, 10 mM sodium fluoride, 2 mM EDTA, 2 mM tetrasodium pyrophosphate, 2 mM sodium orthovanadate, 10 % glycerol, 1 % Triton X-100 plus the protease inhibitors 1 mM phenylmethylsulfonyl fluoride, aprotinin, leupeptin and pepstatin A (1 µg/mL each)], homogenized by a sonifier (five cycles) and centrifuged at 11,000×g for 10 min at 4 °C. Equal amounts of proteins from supernatants were loaded on a SDS/PAGE (sodium dodecyl sulfate-polyacrylamide gel, 10 % for MAPKs and 12.5 % for caspases and Bcl-2 family proteins). Proteins were electrotransferred to poly(vinylidene difluoride) membranes and detected by enhanced chemiluminescence.

#### 5.9. Analysis of mitochondrial membrane potential $\Delta\Psi_m$ and reactive oxygen species (ROS) determination

The mitochondrial membrane potential and intracellular ROS production were determined by flow cytometry using the fluorochromes 5,5',6,6'-tetrachloro-1,1',3,3'-tetraethylbenzimidazolylcarbocyanine iodide (#T4069, Sigma-Aldrich, JC-1, 5 µg/mL) and 2',7'-dichlorodihydrofluorescein diacetate (#35847, Sigma-Aldrich, H<sub>2</sub>-DCF-DA, 10 µM), respectively. Flow cytometric analysis was performed using a BD FACSVerse™ cytometer (BD Biosciences, San Jose, CA, USA) and has been described in detail elsewhere [56].

#### 5.10. Statistical methods

Statistical differences between means were tested using (i) Student's t-test (two samples) or (ii) one-way analysis of variance (ANOVA) (3 or more samples), followed by Tukey's post-hoc tests. A significance level of  $P < 0.05$  was used.

#### CRediT authorship contribution statement

**Juan Perdomo:** Visualization, Investigation, Formal analysis. **Henoc del Rosario:** Visualization, Investigation, Formal analysis. **Ester Saavedra:** Visualization, Investigation, Formal analysis. **Mercedes Said:** Visualization, Investigation, Formal analysis. **Celina García:** Investigation. **Lía Cruces:** Visualization, Investigation, Formal analysis. **Susana Abdala:** Visualization, Investigation, Formal analysis. **Ignacio Brouard:** Writing – review & editing, Writing – original draft, Supervision, Resources, Methodology, Investigation, Data curation, Conceptualization. **José Quintana:** Visualization, Investigation. **Francisco Estévez:** Writing – review & editing, Writing – original draft, Supervision, Resources, Project administration, Methodology, Funding acquisition, Data curation, Conceptualization.

#### Funding

This work was supported by the Agencia Canaria de Investigación, Innovación y Sociedad de la Información (ACIISI, grant number ProID2024010001) and European Regional Development Fund. This research was also funded in part by the Spanish Ministry of Science, Innovation and Universities and the European Regional Development Fund (PGC2018-094503-B-C21 and PGC2018-094503-B-C22). E. Saavedra was funded by Fundación Amurga.

#### Declaration of competing interest

The authors declare the following financial interests/personal relationships which may be considered as potential competing interests: Francisco Estevez reports financial support was provided by Canarian Agency for Research Innovation and Information Society. If there are other authors, they declare that they have no known competing financial interests or personal relationships that could have appeared to influence the work reported in this paper.

#### Acknowledgments

We thank Dr. Jacqueline Bréard and Dr. Lisa Oliver for supplying U-937/Bcl-2 and K-562/ADR, respectively and to Prof. Richard Brown for a linguistic revision of the manuscript.

#### Appendix. ASupplementary data

Supplementary data to this article can be found online at <https://doi.org/10.1016/j.cbi.2025.111877>.



## Data availability

Data will be made available on request.

## References

- [1] D.A. Arber, A. Orazi, R. Hasserjian, J. Thiele, M.J. Borowitz, M.M. Le Beau, C. D. Bloomfield, M. Cazzola, J.W. Vardiman, The 2016 revision to the world health Organization classification of myeloid neoplasms and acute leukemia, *Blood* 127 (2016) 2391–2405, <https://doi.org/10.1182/blood-2016-03-643544>.
- [2] N.S. Wagle, L. Nogueira, T.P. Devasia, A.B. Mariotto, K.R. Yabroff, F. Islami, A. Jemal, R. Alteri, P.A. Ganz, R.L. Siegel, Cancer treatment and survivorship statistics, 2025, *CA Cancer J. Clin.* (2025 May 30), <https://doi.org/10.3322/caac.70011>.
- [3] A.E. Whiteley, T.T. Price, G. Cantelli, D.A. Sipkins, Leukaemia: a model metastatic disease, *Nat. Rev. Cancer* 21 (2021) 461–475, <https://doi.org/10.1038/s41568-021-00355-z>.
- [4] D. Vetrie, G.V. Helgason, M. Copland, The leukaemia stem cell: similarities, differences and clinical prospects in CML and AML, *Nat. Rev. Cancer* 20 (2020) 158–173, <https://doi.org/10.1038/s41568-019-0230-9>.
- [5] H. Dohner, D.J. Weisdorf, C.D. Bloomfield, Acute myeloid leukemia, *N. Engl. J. Med.* 373 (2015) 1136–1152, <https://doi.org/10.1056/NEJMra1406184>.
- [6] H. Kantarjian, T. Kadia, C. DiNardo, N. Dayer, G. Borthakur, E. Jabbour, G. Garcia-Manero, M. Konopleva, F. Ravandi, Acute myeloid leukemia: current progress and future directions, *Blood Cancer J.* 11 (2021) 41, <https://doi.org/10.1038/s41408-021-00425-3>.
- [7] R.L. Siegel, T.B. Kratzer, A.N. Giaquinto, H. Sung, A. Jemal, Cancer statistics, *CA Cancer J. Clin.* 75 (2025) 10–45, <https://doi.org/10.3322/caac.21871>, 2025.
- [8] A. Hochhaus, R.A. Larson, F. Guilhot, J.P. Radich, S. Branford, T.P. Hughes, M. Baccarani, M.W. Deininger, F. Cervantes, S. Fujihara, C.E. Ortmann, H. D. Messen, H. Kantarjian, S.G. O'Brien, B.J. Druker, IRIS Investigators, Long-Term outcomes of imatinib treatment for chronic myeloid leukemia, *N. Engl. J. Med.* 376 (2017) 917–927, <https://doi.org/10.1056/NEJMoa1609324>.
- [9] P. Jain, H.M. Kantarjian, A. Ghorab, K. Sasaki, E.J. Jabbour, G. Noguera Gonzalez, R. Kanagal-Shamanna, G.C. Issa, G. Garcia-Manero, D. Kc, S. Dellasala, S. Pierce, M. Konopleva, W.G. Wierda, S. Verstovsek, N.G. Dayer, T.M. Kadia, G. Borthakur, S. O'Brien, Z. Estrov, F. Ravandi, J.E. Cortes, Prognostic factors and survival outcomes in patients with chronic myeloid leukemia in blast phase in the tyrosine kinase inhibitor era: cohort study of 477 patients, *Cancer* 123 (2017) 4391–4402, <https://doi.org/10.1002/cncr.30864>.
- [10] A.M. Filho, M. Laversanne, J. Ferlay, M. Colombet, M. Piñeros, A. Znaor, D. M. Parkin, I. Soerjomataram, F. Bray, The GLOBOCAN 2022 cancer estimates: data sources, methods, and a snapshot of the cancer burden worldwide, *Int. J. Cancer* 156 (2025) 1336–1346, <https://doi.org/10.1002/ijc.35278>.
- [11] D. Hanahan, Hallmarks of cancer: new dimensions, *Cancer Discov.* 12 (2022) 31–46, <https://doi.org/10.1158/2159-8290.CD-21-1059>.
- [12] B.A. Carneiro, W.S. El-Deiry, Targeting apoptosis in cancer therapy, *Nat. Rev. Clin. Oncol.* 17 (2020) 395–417, <https://doi.org/10.1038/s41571-020-0341-y>.
- [13] I. Vitale, F. Pietrocola, E. Guillaud, S.A. Aaronson, J.M. Abrams, D. Adam, et al., Apoptotic cell death in disease—Current understanding of the NCCD 2023, *Cell Death Differ.* 30 (2023) 1097–1154, <https://doi.org/10.1038/s41418-023-01153-w>.
- [14] D.R. Green, Caspases and their substrates, *Cold Spring Harb. Perspect. Biol.* 14 (2022) a041012, <https://doi.org/10.1101/cshperspect.a041012>.
- [15] B. Tummers, D.R. Green, Caspase-8: regulating life and death, *Immunol. Rev.* 277 (2017) 76–89, <https://doi.org/10.1111/imr.12541>.
- [16] D.J. Newman, G.M. Cragg, Natural products as sources of new drugs over the nearly four decades from 01/1981 to 09/2019, *J. Nat. Prod.* 83 (2020) 770–803, <https://doi.org/10.1021/acs.jnatprod.9b01285>.
- [17] D. Raffa, B. Maggio, M.V. Raimondi, F. Plescia, G. Daidone, Recent discoveries of anticancer flavonoids, *Eur. J. Med. Chem.* 142 (2017) 213–228, <https://doi.org/10.1016/j.ejmech.2017.07.034>.
- [18] C. Forni, M. Rossi, I. Borromeo, G. Feriotta, G. Platamone, C. Tabolacci, C. Mischiati, S. Beninati, Flavonoids: a myth or a reality for cancer therapy? *Molecules* 26 (2021) 3583, <https://doi.org/10.3390/molecules26123583>.
- [19] A.A. WalyEldeen, S. Sabet, H.M. El-Shorbagy, I.A. Abdelhamid, S.A. Ibrahim, Chalcones: promising therapeutic agents targeting key players and signaling pathways regulating the hallmarks of cancer, *Chem. Biol. Interact.* 369 (2023) 110297, <https://doi.org/10.1016/j.cbi.2022.110297>.
- [20] J. Yang, J. Lv, S. Cheng, T. Jing, T. Meng, D. Huo, X. Ma, R. Wen, Recent progresses in chalcone derivatives as potential anticancer agents, *Anti Cancer Agents Med. Chem.* 23 (2023) 1265–1283, <https://doi.org/10.2174/1871520623666230223112530>.
- [21] B. Salehi, C. Quispe, I. Chamkhi, N. El Omari, A. Balahbib, J. Sharifi-Rad, A. Bouayhya, M. Akram, M. Iqbal, A.O. Docea, C. Caruntu, G. Leyva-Gómez, A. Dey, M. Martorell, D. Calina, V. López, F. Les, Pharmacological properties of chalcones: a review of preclinical including molecular mechanisms and clinical evidence, *Front. Pharmacol.* 11 (2021) 592654, <https://doi.org/10.3389/fphar.2020.592654>.
- [22] P.A. Wender, Toward the ideal synthesis and transformative therapies: the roles of step economy and function oriented synthesis, *Tetrahedron* 69 (2013) 7529–7550, <https://doi.org/10.1016/j.tet.2013.06.004>.
- [23] P. Harris, P. Ralph, Human leukemic models of myelomonocytic development: a review of the HL-60 and U937 cell lines, *J. Leukoc. Biol.* 37 (1985) 407–422, <https://doi.org/10.1002/jlb.37.4.407>.
- [24] W. Chanput, V. Peters, H. Wichers, THP-1 and U937 cells, in: K. Verhoeckx, P. Cotter, I. López-Expósito, C. Kleiveland, T. Lea, A. Mackie, T. Requena, D. Swiatecka, H. Wichers (Eds.), *The Impact of Food Bioactives on Health: in Vitro and Ex Vivo Models*, Springer, 2015, pp. 147–159.
- [25] C. Zhuang, W. Zhang, C. Sheng, W. Zhang, C. Xing, Z. Miao, Chalcone: a privileged structure in medicinal chemistry, *Chem. Rev.* 117 (2017) 7762–7810, <https://doi.org/10.1021/acs.chemrev.7b00020>.
- [26] S. Zhuang, J.T. Demirs, I.E. Kochevar, p38 mitogen-activated protein kinase mediates Bid cleavage, mitochondrial dysfunction, and caspase-3 activation during apoptosis induced by singlet oxygen but not by hydrogen peroxide, *J. Biol. Chem.* 275 (2000) 25939–25948, <https://doi.org/10.1074/jbc.M001185200>.
- [27] M. Watabe, H. Kakeya, H. Osada, Requirement of protein kinase (Krs/MST) activation for MT-21-induced apoptosis, *Oncogene* 18 (1999) 5211–5220, <https://doi.org/10.1038/sj.onc.1202901>.
- [28] S.G. Shiah, S.E. Chuang, Y.P. Chau, S.C. Shen, M.L. Kuo, Activation of c-Jun NH2-terminal kinase and subsequent CPP32/Yama during topoisomerase inhibitor beta-lapachone-induced apoptosis through an oxidation-dependent pathway, *Cancer Res.* 59 (1999) 391–398.
- [29] Y.R. Chen, W. Wang, A.N. Kong, T.H. Tan, Molecular mechanisms of c-Jun N-terminal kinase-mediated apoptosis induced by anticarcinogenic isothiocyanates, *J. Biol. Chem.* 273 (1998) 1769–1775, <https://doi.org/10.1074/jbc.273.3.1769>.
- [30] D. Cao, X. Han, G. Wang, Z. Yang, F. Peng, L. Ma, R. Zhang, H. Ye, M. Tang, W. Wu, K. Lei, J. Wen, J. Chen, J. Qiu, X. Liang, Y. Ran, Y. Sang, M. Xiang, A. Peng, L. Chen, Synthesis and biological evaluation of novel pyranochalcone derivatives as a new class of microtubule stabilizing agents, *Eur. J. Med. Chem.* 62 (2013) 579–589, <https://doi.org/10.1016/j.ejmech.2013.01.007>.
- [31] S. Kraege, K. Stefan, S.C. Köhler, M. Wiese, Optimization of acryloylphenylcarboxamides as inhibitors of ABCG2 and comparison with acryloylphenylcarboxylates, *ChemMedChem* 11 (2016) 2547–2558, <https://doi.org/10.1002/cmde.201600455>.
- [32] T. Walle, N. Ta, T. Kawamori, X. Wen, P.A. Tsuji, U.K. Walle, Cancer chemopreventive properties of orally bioavailable flavonoids—methylated versus unmethylated flavones, *Biochem. Pharmacol.* 73 (2007) 1288–1296, <https://doi.org/10.1016/j.bcp.2006.12.028>.
- [33] T. Walle, Methoxylated flavones, a superior cancer chemopreventive flavonoid subclass? *Semin. Cancer Biol.* 17 (2007) 354–362, <https://doi.org/10.1016/j.semcancer.2007.05.002>.
- [34] A.A. Sy-Cordero, T.N. Graf, S.P. Runyon, M.C. Wani, D.J. Kroll, R. Agarwal, S. J. Brantley, M.F. Paine, S.J. Polyak, N.H. Oberlies, Enhanced bioactivity of silybin B methylation products, *Bioorg. Med. Chem.* 21 (2013) 742–747, <https://doi.org/10.1016/j.bmc.2012.11.035>.
- [35] F. Grande, O.I. Parisi, R.A. Mordocco, C. Rocca, F. Puoci, L. Scrivano, A. M. Quintieri, P. Cantafio, S. Perla, A. Brancale, C. Saturnino, M.C. Cerra, M. S. Sinicropi, T. Angelone, Quercetin derivatives as novel antihypertensive agents: synthesis and physiological characterization, *Eur. J. Pharm. Sci.* 82 (2016) 161–170, <https://doi.org/10.1016/j.ejps.2015.11.021>.
- [36] M.K. Kim, K.S. Park, C. Lee, H.R. Park, H. Choo, Y. Chong, Enhanced stability and intracellular accumulation of quercetin by protection of the chemically or metabolically susceptible hydroxyl groups with a pivaloxymethyl (POM) promoiety, *J. Med. Chem.* 53 (2010) 8597–8607, <https://doi.org/10.1021/jm101252m>.
- [37] E. Saavedra, H. Del Rosario, I. Brouard, J. Quintana, F. Estévez, 6'-Benzyloxy-4-bromo-2'-hydroxychalcone is cytotoxic against human leukaemia cells and induces caspase-8- and reactive oxygen species-dependent apoptosis, *Chem. Biol. Interact.* 298 (2019) 137–145, <https://doi.org/10.1016/j.cbi.2018.12.010>.
- [38] L. Dubrez, F. Goldwasser, P. Genne, Y. Pommier, E. Solary, The role of cell cycle regulation and apoptosis triggering in determining the sensitivity of leukemic cells to topoisomerase I and II inhibitors, *Leukemia* 9 (1995) 1013–1024.
- [39] R.M. Gangemi, M. Tiso, C. Marchetti, A.B. Severi, M. Fabbri, Taxol cytotoxicity on human leukemia cell lines is a function of their susceptibility to programmed cell death, *cancer Chemother. Pharmacol.* 36 (1995) 385–392, <https://doi.org/10.1007/BF00686187>.
- [40] S.H. Kaufmann, S. Desnoyers, Y. Ottaviano, N.E. Davidson, G.G. Poirier, Specific proteolytic cleavage of poly(ADP-ribose) polymerase: an early marker of chemotherapy-induced apoptosis, *Cancer Res.* 53 (1993) 3976–3985.
- [41] A. McGahan, R. Bissonnette, M. Schmitt, K.M. Cotter, D.R. Green, T.G. Cotter, BCR-ABL maintains resistance of chronic myelogenous leukemia cells to apoptotic cell death, *Blood* 83 (1994) 1179–1187.
- [42] S. Ray, G. Bullock, G. Nuñez, C. Tang, A.M. Ibrado, Y. Huang, K. Bhalla, Enforced expression of Bcl-XS induces differentiation and sensitizes chronic myelogenous leukemia-blast crisis K562 cells to 1-beta-D-arabinofuranosylcytosine-mediated differentiation and apoptosis, *Cell Growth Differ.* 7 (1996) 1617–1623.
- [43] N. Margolin, S.A. Raybuck, K.P. Wilson, W. Chen, T. Fox, Y. Gu, D.J. Livingston, Substrate and inhibitor specificity of interleukin-1 beta-converting enzyme and related caspases, *J. Biol. Chem.* 272 (1997) 7223–7228, <https://doi.org/10.1074/jbc.272.11.7223>.
- [44] S.A. Amundson, T.G. Myers, D. Scudiero, S. Kitada, J.C. Reed, A.J. Fornace Jr., An informatics approach identifying markers of chemosensitivity in human cancer cell lines, *Cancer Res.* 60 (2000) 6101–6110.
- [45] J.N. Moloney, T.G. Cotter, ROS signalling in the biology of cancer, *Semin. Cell Dev. Biol.* 80 (2018) 50–64, <https://doi.org/10.1016/j.semdb.2017.05.023>.
- [46] S.B. Panina, N. Baran, F.H. Brasil da Costa, M. Konopleva, N.V. Kirienko, A mechanism for increased sensitivity of acute myeloid leukemia to mitotoxic

- drugs, *Cell Death Dis.* 10 (2019) 617, <https://doi.org/10.1038/s41419-019-1851-3>.
- [47] Q. Peng, Z. Deng, H. Pan, L. Gu, O. Liu, Z. Tang, Mitogen-activated protein kinase signaling pathway in oral cancer, *Oncol. Lett.* 15 (2018) 1379–1388, <https://doi.org/10.3892/ol.2017.7491>.
- [48] E.V. Stoyanov, Y. Champavier, A. Simon, J.P. Basly, Efficient liquid-phase synthesis of 2'-hydroxychalcones, *Bioorg. Med. Chem. Lett.* 12 (2002) 2685–2687, [https://doi.org/10.1016/s0960-894x\(02\)00553-x](https://doi.org/10.1016/s0960-894x(02)00553-x).
- [49] P.L. Zhao, C.L. Liu, W. Huang, Y.Z. Wang, G.F. Yang, Synthesis and fungicidal evaluation of novel chalcone-based strobilurin analogues, *J. Agric. Food Chem.* 55 (2007) 5697–5700, <https://doi.org/10.1021/jf071064x>.
- [50] H. del Rosario, E. Saavedra, I. Brouard, D. González-Santana, C. García, E. Spínola-Lasso, C. Tabraue, J. Quintana, F. Estévez, Structure-activity relationships reveal a 2-furoyloxchalcone as a potent cytotoxic and apoptosis inducer for human U-937 and HL-60 leukaemia cells, *Bioorg. Chem.* 127 (2022) 105926, <https://doi.org/10.1016/j.bioorg.2022.105926>.
- [51] M. Liu, P. Wilairat, S.L. Croft, A.L. Tan, M.L. Go, Structure-activity relationships of antileishmanial and antimalarial chalcones, *Bioorg. Med. Chem.* 11 (2003) 2729–2738, [https://doi.org/10.1016/s0968-0896\(03\)00233-5](https://doi.org/10.1016/s0968-0896(03)00233-5).
- [52] R.S. Joshi, P.G. Mandhane, S.D. Diwakar, S.K. Dabhade, C.H. Gill, Synthesis, analgesic and anti-inflammatory activities of some novel pyrazolines derivatives, *Bioorg. Med. Chem. Lett.* 20 (2010) 3721–3725, <https://doi.org/10.1016/j.bmcl.2010.04.082>.
- [53] B.H. Kim, S.N. Hong, S.K. Ye, J.Y. Park, Evaluation and optimization of the anti-melanogenic activity of 1-(2-Cyclohexylmethoxy-6-hydroxy-phenyl)-3-(4-hydroxymethyl-phenyl)-propenone derivatives, *Molecules* 24 (2019) 1372, <https://doi.org/10.3390/molecules24071372>.
- [54] J.A. Smith, D.J. Maloney, S.M. Hecht, D.A. Lannigan, Structural basis for the activity of the RSK-specific inhibitor, SL0101, *Bioorg. Med. Chem.* 15 (2007) 5018–5034, <https://doi.org/10.1016/j.bmc.2007.03.087>.
- [55] T. Mosmann, Rapid colorimetric assay for cellular growth and survival: application to proliferation and cytotoxicity assays, *J. Immunol. Methods* 65 (1983) 55–63, [https://doi.org/10.1016/0022-1759\(83\)90303-4](https://doi.org/10.1016/0022-1759(83)90303-4).
- [56] F. Estévez-Sarmiento, E. Hernández, I. Brouard, F. León, C. García, J. Quintana, F. Estévez, 3'-Hydroxy-3,4'-dimethoxyflavone-induced cell death in human leukaemia cells is dependent on caspases and reactive oxygen species and attenuated by the inhibition of JNK/SAPK, *Chem. Biol. Interact.* 288 (2018) 1–11, <https://doi.org/10.1016/j.cbi.2018.04.006>.